ABSTRACT

NELSON, JILL SERENA. Numerical Investigation of Air-Sea Interactions During Winter Extratropical Storms. (Under the direction of Dr. Ruoying He.)

A high-resolution, regional coupled atmosphere-ocean model is used to investigate Gulf Stream-induced surface wind convergence (SWC) during an extratropical cyclone (ETC) outbreak off the east coast of the United States in January 2005. The coupled model realistically reproduces the strong storm winds, fluctuations in sea level pressure (SLP), persistent ocean cooling, and upper ocean temperature structures measured by marine buoys and an ocean glider during the study period (13-31 January 2005). Numerical model analysis shows a well-defined band of synoptic mean surface wind convergence aligned over the Gulf Stream during the ETC outbreak. Both a theoretical model of the marine atmospheric boundary layer (MABL) and coupled model simulations show the synoptic mean SWC is highly correlated to Laplacian of sea level pressure (r=0.82) and the inverse Laplacian of sea surface temperature (r=0.52). Strong SWC induces upward vertical motions throughout the MABL and enhances ocean heat loss, supporting rapid ETC intensification off the eastern U.S. seaboard. In simulations without dynamic coupling between the atmosphere and ocean models, the relationship between synoptic mean SWC and the Laplacian of SLP and the inverse Laplacian of ocean temperatures does not hold.

The 22-23 January 2005 winter storm is selected as a case study to further examine air-sea interactions within a rapidly intensifying ETC. The 22-23 January storm induced large (>1000 W m^{-2}) total sensible and latent heat flux as cold, dry air swept across the warm waters in the western Atlantic Ocean, resulting in a ~2 °C decrease in sea surface temperature (SST). The heat loss in the upper 100-m of the Gulf Stream over the storm period was dominated by surface heat fluxes out of the ocean. In order to improve ETC predictions and

regional coastal wind and wind energy potential assessment in general, dynamic air-sea interactions affecting momentum and buoyancy flux exchanges have to be accurately accounted for in a coupled ocean-atmosphere modeling framework.

Numerical Investigation of Air-Sea Interactions During Winter Extratropical Storms

by
Jill Serena Nelson

A thesis submitted to the Graduate Faculty of
North Carolina State University
in partial fulfillment of the
requirements for the degree of
Master of Science

Marine, Earth, and Atmospheric Sciences

Raleigh, North Carolina

2011

APPROVED BY:

_____	_____
Dr. Ruoying He Committee Chair	Dr. John Bane

_____
Dr. Ping-Tung Shaw

BIOGRAPHY

Jill Nelson was born on 18 April 1987 in Minneapolis, Minnesota, and shortly thereafter her family moved to the Mississippi Gulf Coast. Her interest in meteorology as a career path began after her community was destroyed by Hurricane Katrina in 2005. She attended Mississippi State University in Starkville, Mississippi, from 2005 to 2009 and graduated with a bachelor's degree in Operational Meteorology. In the summer after graduation, she went storm chasing across the Great Plains with a small group of meteorology students and professors from Mississippi State and saw her first and only tornado in an open field in Oklahoma. Later that year she enrolled in the Marine Sciences program at North Carolina State University, joining the Ocean Observing and Modeling Group. At the time of her graduation from NC State, Jill had accepted a job offer with a small private firm providing oceanographic services supporting the needs of the offshore oil and gas industry.

ACKNOWLEDGMENTS

I would like to thank Dr. Ruoying He for his guidance and support as my research advisor during my two years at NCSU. I thank Dr. John Bane of UNC for scientific guidance and many enlightening discussions, and Dr. Ping-Tung Shaw for serving on my committee. I thank Dr. John Warner of USGS for leading the effort in developing and testing the COAWST modeling system.

Thanks to the entire Ocean Observing and Modeling team for making NCSU a great place to work: Joe Zambon, Yizhen Li, Ke Chen, Hui Qian, Yanlin Gong, Zhigang Yao, Yao Zhao, Zuo Xue, and Kyung Hoon Hyun.

A special thanks goes to my family for all their love and support over the years. I thank my friends in North Carolina and Mississippi who have cheered me on through this journey. Most of all, thanks to Mitch Storie for his love, understanding, and encouragement.

I am grateful for research funding support provided by NSF and ONR through grants OCE-0927470 and N00014-06-1-0739, respectively.

TABLE OF CONTENTS

LIST OF TABLES

LIST OF FIGURES

CHAPTER 1

CHAPTER 2

CHAPTER 3

CHAPTER 1

Introduction

1. Winter Extratropical Cyclones

Winter extratropical cyclones (ETCs) are synoptic low pressure systems (**Figure 1)** that regularly occur between October and April in the eastern United States. The majority of ETCs originate in the southeastern U.S. and track southwest to northeast following the eastern coastline and finally dissipating near Iceland [*Zishka and Smith*, 1980; *Hirsh et al.*, 2001]. Typical mid-latitude cyclones (those forming in the lee of the Rocky Mountains and following a more northerly track) can also generate a secondary area of low pressure off the northeastern coast which often develop rapidly (over several hours) into mature cyclones [*Hirsch et al.*, 2001]. An average of 12 ETCs impact the U.S. east coast each winter season, deepening to about 993 mb and producing winds greater than 20 ms^{-1} [*Hirsch et al.*, 2001].

Severe ETCs, commonly known as winter storms or Nor'easters, are most common in January [*Colucci*, 1976; *Zishka and Smith*, 1980]. The narrow coastal zone between Cape Hatteras, North Carolina, and the Gulf Stream is a favorable region for "explosive" cyclogenesis [*Reitan*, 1974; *Colucci*, 1976; *Sanders and Gyakum*, 1980; *Zishka and Smith*, 1980; *Whittaker and Horn*, 1981; *Davis et al.*, 1993]. Rapidly intensifying "bomb" cyclones (those defined as having central pressure deepening rates of at least 1 mb hr^{-1} for 24 hours [*Sanders and Gyakum*, 1980]) form or offshore redevelopment occurs within this small region as cold, dry Arctic air sweeps eastward across the U.S. coastline and over the

relatively warm (20 to 24 °C) Atlantic Ocean, destabilizing the atmosphere and inducing large surface heat and moisture fluxes out of the ocean. Rapid deepening at the surface is often accompanied by an upper level forcing (e.g. 500 mb jet and trough) (**Figure 1**). Providing accurate forecasts of explosive east coast cyclogenesis remains a challenging problem due to the complex air-sea interactions within the storm and the relationship to the large-scale atmospheric circulation.

Winter storms cause widespread economic, societal, and environmental impacts. Heavy snow and ice accumulations from winter storms can bring the northeast U.S. to a standstill for several days. Businesses and schools are forced to shut down until roads can be cleared of snow and debris and power is restored and the offshore industry halts operations until it is safe to travel the seas. The combination of strong winds and extreme cold can lead to dangerous and potentially fatal wind chills. Coastal areas are impacted by severe beach erosion from long periods of strong winds, waves, and storm surge.

2. Ocean Regimes off the U.S. East Coast

The most important feature off the east coast of the United States is the Gulf Stream (GS), a surface-intensified warm (24 °C) western boundary current that flows northward at up to 2 m s^{-1} in close proximity to the southeastern U.S. continental margin until Cape Hatteras where it separates from the coast and heads east across the Atlantic Ocean (**Figure 2**) [*Phillips and Gasparovic*, http://fermi.jhuapl.edu/student/phillips]. The Gulf Stream is the western boundary of the North Atlantic Subtropical Gyre (NASG) that circulates clockwise around the Sargasso Sea in the middle of the Atlantic Ocean. The GS is about 100 km wide

and extends about 1000 m deep. In winter, the shoreward edge of the GS (e.g. the Gulf Stream Front) is several degrees warmer than surrounding waters and as much as 20 °C warmer than land. As such, strong cross-shelf SST gradients exist off the southeastern U.S. and especially near Cape Hatteras where the GS has its most onshore position.

The eastern continental shelf of the United States can be divided into two sections: the Middle Atlantic Bight (MAB) from Cape Hatteras to Massachusetts and the South Atlantic Bight (SAB) from Cape Hatteras to Florida (**Figure 2**).

The MAB continental shelf is broad and shallow, increasing from 30 km wide and 40 m deep near Cape Hatteras to 100 km wide and 100 m deep in the northern MAB [*Lentz*, 2008]. The shelfbreak front separates cool, fresh shelf water from warmer, salty slope water [*Linder and Gawarkiewicz*, 1998]. The annual mean depth-averaged flow is 3-10 cm s^{-1} towards the south (**Figure 3**) [*Lentz*, 2008]. In winter, cold air temperatures and strong northwesterly wind stress vertically mix the upper ocean, whereas in summer, warm air temperatures and weak southwesterly wind stress stratify the water column.

The width of the SAB continental shelf ranges from 50 km off Florida, to 120 km off Georgia and South Carolina, and to 30 km off Cape Hatteras. The SAB can be further subdivided into the inner, middle, and outer shelves based on the bathymetry and dominant physical forcing mechanisms in each region (**Figure 4**).

The inner shelf (0-20 m) is dominated by large freshwater discharge from several rivers along the SAB which generates a well-defined low-salinity, stratified, alongshore front throughout the year [*Oey*, 1986; *Lee et al.*, 1985]. Surface flow correlates with local wind stress, which is southward in winter and northward in summer.

Dynamics of the middle shelf (20-40 m) are primarily forced by tides and local winds, though lateral movements of the Gulf Stream through Ekman transport can also play a role especially during strong winter storms [*Lee et al.*, 1985]. Like the MAB, stratification on the middle SAB shelf varies seasonally. Strong northerly winds in the winter months help to cool and mix the water vertically until spring and summer when the combination of the cross-shelf transport of freshwater from the coast, surface heat flux, and a reduction in mixing stratifies the water column [*Lee et al.*, 1985].

The outer shelf (depths > 40 m) is strongly coupled to the Gulf Stream, especially in the northern SAB where the Gulf Stream becomes unstable due to its own dynamics. The Gulf Stream is deflected offshore by the Charleston Bump (a sharp rise in the bottom topography located near 32°N 79°W), resulting in the generation of eddies (lengths on the order of 300 km), filaments (on the order of 200 km), and meanders (on the order of 100 km) on the shoreward side of the Stream which propagate downstream and intrude on the SAB shelf [*Lee et al.*, 1991]. Northerly (southerly) wind stress in the winter (summer) can cause lateral displacements of the Gulf Stream on the order of 40 km from its mean position which also influence the temperature and flow regimes of the outer shelf [*Bane and Brooks*, 1979; *Lee et al.*, 1991].

3. Research Background

The Genesis of Atlantic Lows (GALE) field program was conducted from 15 January to 15 March 1986. It was a large, multi-institutional effort to measure concurrent atmospheric and oceanic conditions at high spatial and temporal resolution in the vicinity of

the Gulf Stream where "explosively" intensifying ETCs frequently develop [*Dirks et al.*, 1988]. Some of the program's main objectives were to gain a better understanding of the mesoscale air-sea interaction processes within winter extratropical cyclones that lead to such rapid intensification of east coast ETCs and to develop and test new models to improve predictions of explosive offshore cyclogenesis.

Observations made during GALE revealed that feedbacks over the Gulf Stream have a strong impact on the marine atmospheric boundary layer (MABL) during the ETC intensification and on the upper ocean during the subsequent cold air outbreak. Studies using GALE data identified excessive ocean-to-atmosphere heat fluxes and surface wind convergence over the Gulf Stream as two air-sea interactions important for ETC generation off the U.S. eastern seaboard.

During cold air outbreaks, the observed total ocean-to-atmosphere heat flux can exceed 1000 W m^{-2} within the GS due to large air-sea temperature and humidity differences, which is several times larger than the maximum climatological fluxes [*Bane and Osgood*, 1989; *Wayland and Raman*, 1994]. Surface heat fluxes are important for providing heat and moisture to developing storms [*Holt and Raman*, 1990; *Warner et al.*, 1990]. Excessive heat flux over the Gulf Stream during cold air outbreaks affects surface wind and pressure fields. *Xue et al.* [2000] observed that surface winds increase by as much as 75% over the Gulf Stream due to the large heat flux during a cold air outbreak. *Li et al.* [2002] investigated spatial and temporal heat flux distributions during the passage of a winter storm and found that the central pressure dropped sharply as the cyclone encountered the large heat flux gradients at the shoreward side of the Gulf Stream. The oceanic response to such strong

atmospheric forcing is a 1-2 °C temperature decrease and about a 35-m deepening of the ocean mixed layer over one storm period [*Bane and Osgood*, 1989]. *Xue et al.* [1995] found that the Gulf Stream heat budget is balanced by ocean-to-atmosphere heat flux and a decrease in heat content in the upper ocean.

During GALE, *Reddy and Raman* [1994] observed the acceleration of low-level winds toward the Gulf Stream and the formation of a surface convergence zone near the largest SST gradients. The two-dimensional numerical analysis of *Huang and Raman* [1988, 1991] reproduced the low-level wind convergence zone over the Gulf Stream, consistent with GALE observations, and showed that such convergence induces mesoscale atmospheric circulations up to the height of the MABL.

To better understand and quantify air-sea interactions during ETCs, this thesis research applies a newly developed air-sea coupled model in a case study of winter cyclones in January 2005. Chapter 2 of this thesis provides analyses of air-sea interactions and heat exchanges during the 22-23 January 2005 bomb cyclone off the United States east coast diagnosed from a coupled air-sea model. The impact of the Gulf Stream on synoptic mean surface wind convergence during the 13-31 January 2005 extratropical cyclone outbreak is examined in Chapter 3, followed by a research summary in Chapter 4.

REFERENCES

Bane, J. M., and D. A. Brooks (1979), Gulf Stream meanders along the continental margin from the Florida Straits to Cape Hatteras, *Geophys. Res. Lett.*, *6*, 280-282.

Bane, J. M., and K. E. Osgood (1989), Wintertime air-sea interaction processes across the Gulf Stream, *J. Geophys. Res.*, *94*, 10755-10772.

Colucci, S. J. (1976), Winter cyclone frequencies over the eastern United States and adjacent western Atlantic, 1964-1973, *Bull. Am. Meteor. Soc.*, *57*(5), 548-553.

Davis, R. E., R. Dolan, and G. Demme (1993), Synoptic climatology of Atlantic coast northeasters, *Int. J. Climatol.*, *13*, 171-189.

Dirks, R. A., J. P. Kuettner, and J. A. Moore (1988), Genesis of Atlantic Lows Experiment (GALE): An overview, *Bull. Am. Meteor. Soc.*, *69*(2), 148-160.

Hadlock, R., and C. W. Kreitzberg (1988), The Experiment on Rapidly Intensifying Cyclones over the Atlantic (ERICA) field study: Objectives and plans, *B. Am. Meteorol. Soc.*, *69*(11), 1309-1320.

Hirsch, M. E., A. T. DeGaetano, and S. J. Colucci (2001), An east coast winter storm climatology, *J. Climate*, *14*, 882-899.

Holt, T. R., and S. Raman (1990), Marine boundary-layer structure and circulation in the region of offshore redevelopment of a cyclone during GALE, *Mon. Weather Rev.*, 120, 17-39.

Huang, C.-Y., and S. Raman (1988), A numerical modeling study of the marine boundary layer over the Gulf Stream during cold air advection, *Bound.-Layer Meteor.*, *45*, 251-290.

Huang, C.-Y., and S. Raman (1991), Numerical simulation of January 28 cold air outbreak during GALE part II: The mesoscale circulation and marine boundary layer, *Bound.-Layer Meteor.*, *56*, 51-81.

Lee, T. N., J. Yoder, and L. Atkinson (1991), Gulf Stream frontal eddy influence on the productivity of the southeast U.S. continental shelf, *J. Geophys. Res.*, *96*, 22191-22205.

Lee, T. N., V. Kourafalou, J. D. Wang, W. J. Ho, J. O. Blanton, L. P. Atkinson, and L. J. Pietrafesa (1985), Shelf circulation from Cape Canaveral to Cape Fear during winter, *Oceanography of the Southeastern U.S. Continental Shelf, Coastal and Estuarine Sciences 2,* edited by L. P. Atkinson et al., AGU, Washington D.C., 33-62.

Lentz, S. J. (2008), Observations and a model of the mean circulation over the Middle Atlantic Bight continental shelf, *J. Phys. Oceanogr., 38,* 1203-1221.

Linder, C. A., and G. Gawarkiewicz (1998), A climatology of the shelfbreak front in the Middle Atlantic Bight, *J. Geophys. Res., 103,* 18405-18423.

Li, Y., H. Xue, and J. M. Bane (2002), Air-sea interactions during the passage of a winter storm over the Gulf Stream: A three-dimensional coupled atmosphere-ocean model study, *J. Geophys. Res., 107,* 1-13.

Oey, L. W. (1986), The formation and maintenance of density fronts on the U.S. southeastern continental shelf during winter, *J. Phys. Oceanogr., 16,* 1121-1135.

Phillips, P., and R. Gasparovic (retrieved 2011), The Gulf Stream, US Naval Academy and Johns Hopkins University, WWW page: http://fermi.jhuapl.edu/student/phillips.

Reddy, N. C., and S. Raman (1994), Observations of a mesoscale circulation over the Gulf Stream region, *Global Atmos. Ocean Syst., 2,* 21-39.

Reitan, C. H. (1974), Frequencies of cyclones and cyclogenesis for North America, 1951-1970, *Mon. Weather Rev., 102,* 861-868.

Sanders, F., and J. R. Gyakum (1980), Synoptic-dynamic climatology of the "bomb", *Mon. Weather Rev., 108,* 1589-1606.

Warner, T. T., M. N. Lakhtakia, J. D. Doyle, and R. A. Pearson (1990), Marine atmospheric boundary layer circulations forced by Gulf Stream sea surface temperature gradients, *Mon. Weather Rev., 118,* 309-323.

Wayland, R. J., and S. Raman (1994), Structure of the marine atmospheric boundary layer during two cold air oubreaks of varying intensities: GALE 1986, *Bound.-Layer Meteor., 71,* 43-66.

Whittaker, L. M., and L. H. Horn (1981), Geographical and seasonal distribution of North American cyclogenesis, 1958-1977, *Mon. Weather Rev., 109,* 2312-2322.

Xue, H., J. M. Bane, and L. M. Goodman (1995), Modification of the Gulf Stream through strong air-sea interactions in winter: Observations and numerical simulations, *J. Phys. Oceanogr.*, *25*, 533-557.

Xue, H., Z. Pan, and J. M. Bane (2000), A 2D coupled atmosphere-ocean model study of air-sea interactions during a cold air outbreak over the Gulf Stream, *Mon. Weather Rev.*, *128*, 973-996.

Zishka, K. M., and P. J. Smith (1980), The climatology of cyclones and anticyclones over North America and surrounding ocean environs for January and July, 1950-77, *Mon. Weather Rev.*, *108*(4), 387-401.

FIGURES

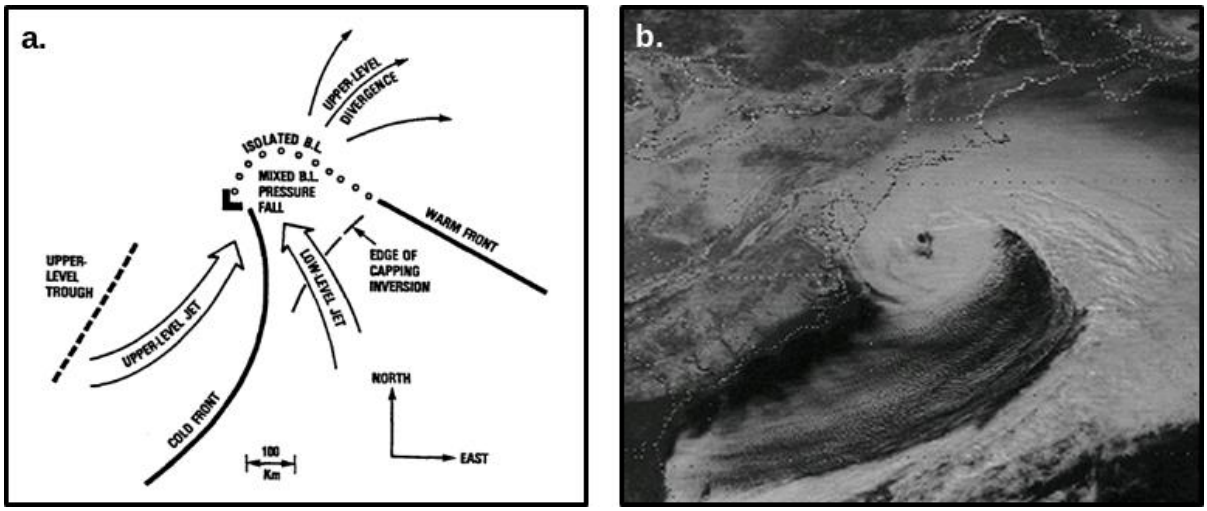

Figure 1. Schematic of a synoptic low pressure system with surface fronts and upper level features [*Hadlock and Kreitzberg*, 1988] (a) and satellite imagery of an extratropical cyclone off the east coast of the U.S. (b, photo courtesy of the University of Colorado).

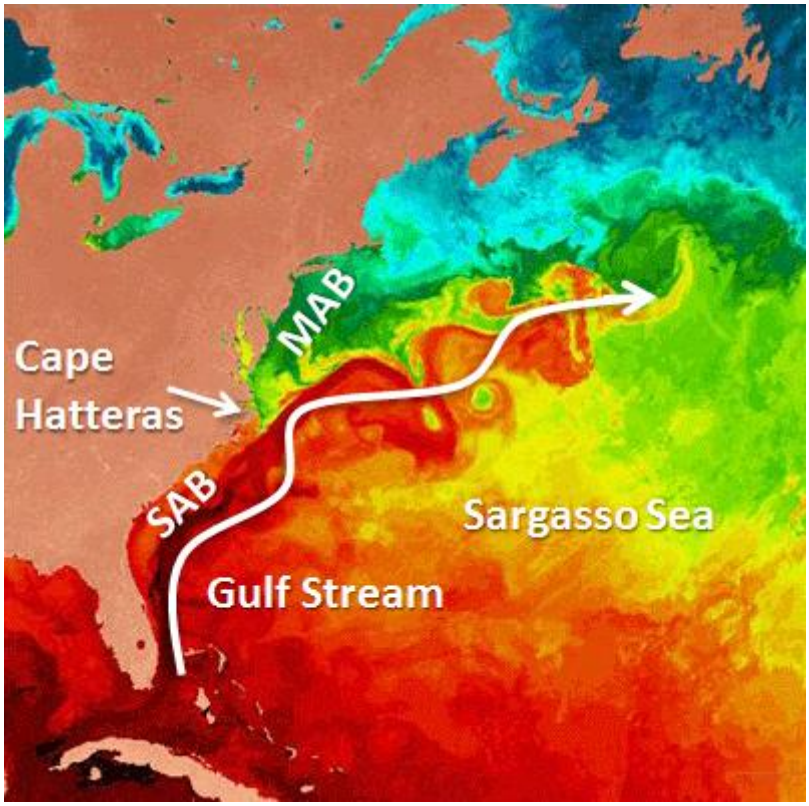

Figure 2. Sea surface temperatures and ocean regimes in the Atlantic Ocean off the U.S. east coast.

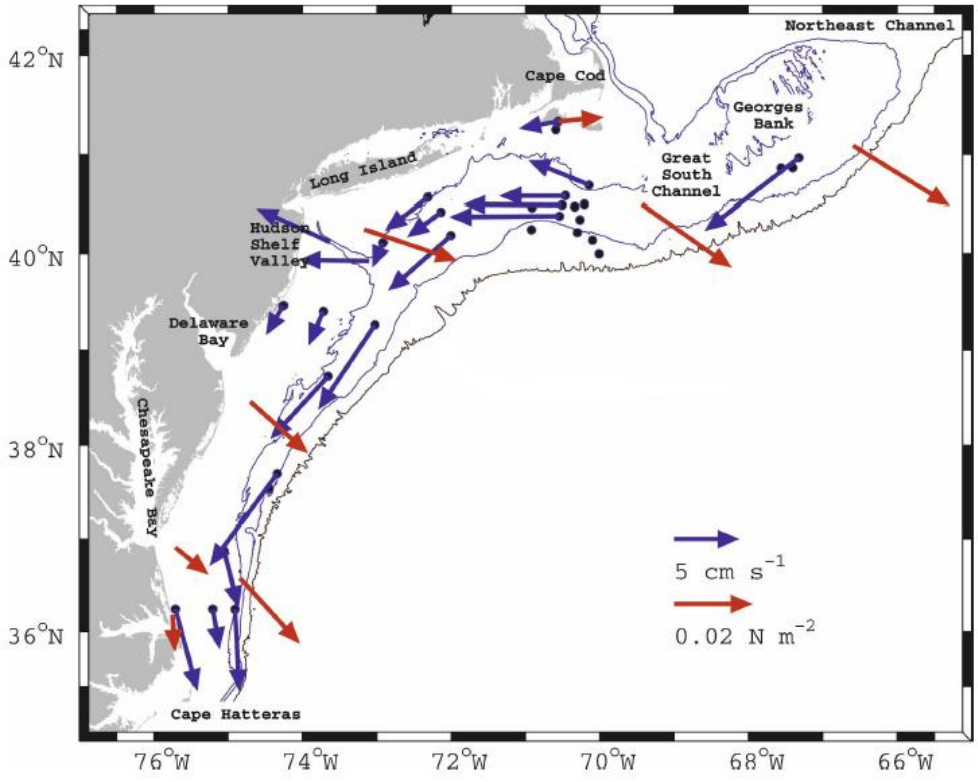

Figure 3. Map of the Middle Atlantic Bight showing the climatological mean depth-averaged current vectors (blue), mean wind stress vectors (red), and the 50-, 100-, and 1000-m isobaths [*Lentz et al.*, 2001].

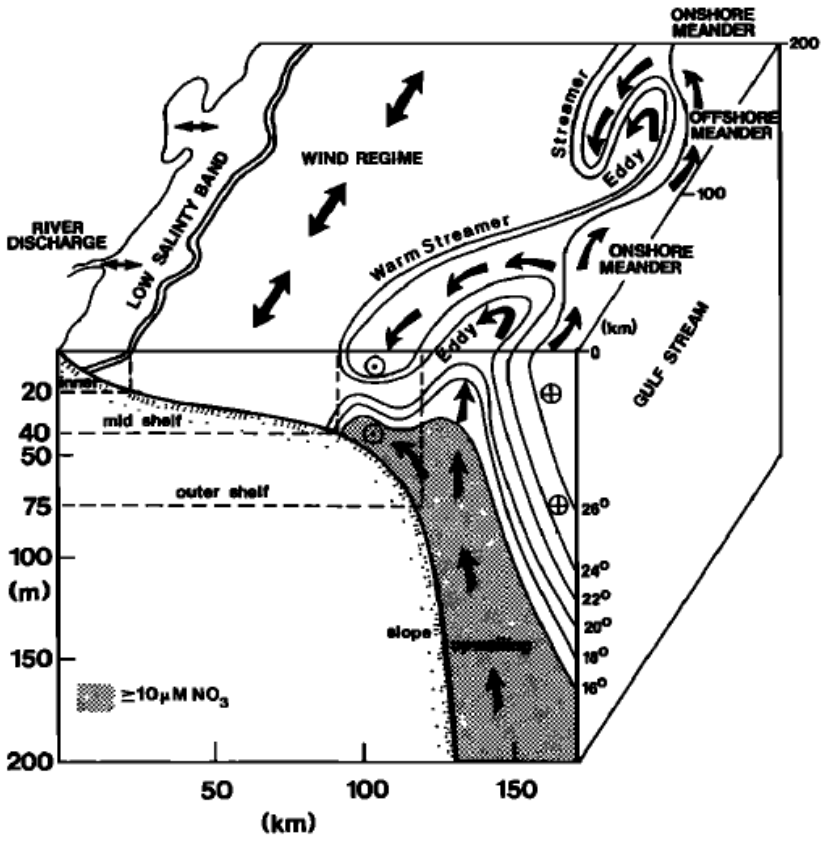

Figure 4. Schematic of the physical forcing mechanisms and flow regimes in the South Atlantic Bight [*Lee et al.*, 1991].

CHAPTER 2

Air-Sea Interactions During Strong Winter Extratropical Storms

Jill S. Nelson and Ruoying He

Dept. of Marine, Earth, and Atmospheric Sciences

North Carolina State University

Raleigh, North Carolina, USA

Manuscript submitted to

Dynamics of Atmospheres and Oceans

Abstract

A high-resolution, regional atmosphere-ocean coupled model is used to investigate strong air-sea interactions during a rapidly developing extratropical cyclone (ETC) off the east coast of the United States on 22-23 January 2005. In this two-way coupled model system, wind stress and net heat flux from the Weather Research and Forecasting (WRF) atmosphere model and sea surface temperature (SST) from the Regional Ocean Modeling System (ROMS) are exchanged via the Model Coupling Toolkit (MCT). Model validations against in-situ buoy and ocean glider data show that the coupled model accurately reproduces the strong storm winds, fluctuations in sea level pressure, persistent ocean cooling, and upper ocean temperature structures observed off the U.S. east coast in January 2005. Vertical profiles of simulated air temperature and winds in the marine atmospheric boundary layer

(MABL) and temperature variations in the upper ocean during a three-day storm period are examined at various cross-shelf transects. It is found that air-sea interactions near the Gulf Stream are important for generating and sustaining the ETC. In particular, locally enhanced winds over the sharp SST front induce large surface heat fluxes which cool the upper ocean by up to 2 °C. Detailed heat budget analyses show the ocean-to-atmosphere heat flux dominates the upper ocean heat content variations. Our results clearly show that energetic air-sea interactions affecting momentum and buoyancy flux exchanges in ETCs need to be accounted for in a coupled atmosphere-ocean modeling framework.

1. Introduction

Severe winter storms off the U.S. east coast, commonly known as Nor'easters, are most frequent and intense in January [*Colucci*, 1976; *Zishka and Smith*, 1980; *Hirsch et al.*, 2001]. These fast-moving, synoptic low-pressure systems often bring heavy precipitation, strong northeasterly winds, and bitterly cold temperatures to the mid-Atlantic states. The impacts of these storms can be especially devastating to the densely populated metropolitan areas in the Northeast, as well as coastal areas due to storm-induced waves, sea level rise, and severe beach erosion. Winter extratropical storms arguably cause more damage to the U.S. east coast than tropical storms and hurricanes due to their high frequency between October and April, long duration, and wide-spread societal, economic, and environmental impacts [*DeGaetano*, 2008]. Several climatological studies have indicated that the most favorable region for winter cyclone occurrence and intensification is parallel to the U.S./Canada east coast, stretching from the North Carolina coast to Newfoundland [*Colucci*, 1976; *Sanders and Gyakum*, 1980; *Zishka and Smith*, 1980]. Particularly strong "bomb" cyclones (those with central pressure deepening rates of at least 24 mb day^{-1} [*Sanders and Gyakum*, 1980]) often develop near Cape Hatteras in the surface convergence zone between a cold, dry Arctic air mass and the relatively warm marine air (>20 °C) overlying the Gulf Stream.

The Gulf Stream is a warm (24 °C), swift western boundary current that meanders northward along the southeastern U.S. continental margin to Cape Hatteras where it then separates from the margin and travels eastward across the Atlantic Ocean (**Figure 1**). It is roughly 100 km wide and 1000 m deep. The continental shelf ocean north (south) of Cape

Hatteras is known as the Middle (South) Atlantic Bight (hereafter called the MAB and SAB). Seaward of the Gulf Stream is a relatively warm anti-cyclonic gyre known as the Sargasso Sea. In winter, the cross-shelf sea surface temperature (SST) gradient is larger in the SAB than in the MAB because of the close proximity (<100 km) of the Gulf Stream to land. Sharp changes in SST off the southeastern U.S. coast and large ocean-to-atmosphere heat fluxes from the Gulf Stream induce energetic air-sea interactions which rapidly modify the marine atmospheric boundary layer (MABL) and influence storm development [*Small et al*., 2008].

Understanding the complex air-sea interactions that occur during the strong extratropical cyclones (ETCs) that regularly form over the U.S. east coast in winter and intensify explosively as they track across the western Atlantic Ocean was the core objective of the Genesis of Atlantic Lows Experiment (GALE). The GALE field program was conducted from 15 January to 15 March 1986 [*Dirks et al*, 1988]. This program was designed to measure concurrent atmospheric and oceanic conditions at high spatial and temporal frequency so as to resolve modifications to the MABL and the ocean mixed layer associated with the passage of an ETC. *Reddy and Raman* [1994] observed during GALE the formation of a surface convergence zone as low-level winds accelerated toward the Gulf Stream and induced a mesoscale circulation in the MABL. Both *Wayland and Raman* [1994] and *Bane and Osgood* [1989] observed near-surface turbulent atmospheric heat fluxes in excess of 1000 W m^{-2} over the Gulf Stream due to large air-sea temperature and humidity differences during the 25-30 January 1986 storm and cold air outbreak. *Bane and Osgood* [1989] also documented a 1-2 °C decrease in upper ocean temperature and a 35-m deepening

of the ocean mixed layer over the 5-day storm period. Numerical model analysis of *Xue et al.* [1995] showed that the decrease in heat content of the Gulf Stream mixed layer is balanced by the large heat flux from the ocean to the atmosphere during the same late January 1986 cold air outbreak.

Recent advancements in regional coupled models now allow more detailed analysis on atmosphere-ocean feedbacks during ETCs. In this study, we utilize the newly-developed Coupled-Ocean-Atmosphere-Wave-Sediment-Transport (COAWST) modeling system to assess strong air-sea interactions during an intense east coast winter storm. We focus on a "bomb" ETC that formed offshore near Cape Hatteras and rapidly developed into a strong cyclone on 23 January 2005. A detailed description of the three-dimensional atmosphere-ocean coupled modeling system and its model configuration are given in Section 2. A synoptic description of ETCs in January 2005 is given in Section 3. Section 4 presents model validations against in-situ observations from marine meteorological buoys and ocean glider data. Discussions on the coupled model results, including the feedbacks between the MABL and the upper ocean and the oceanic heat budget analysis are given in Section 5, followed by conclusions in Section 6.

2. Model and Data

2.1 Coupled Model Description

The Coupled-Ocean-Atmosphere-Wave-Sediment-Transport (COAWST) modeling system was developed to investigate storm impacts on coastal ocean environments [*Warner et al.*, 2010]. The fully coupled system consists of four model components: the Regional

Ocean Modeling System (ROMS) [*Shchepetkin and McWilliams*, 2005], the Weather Research and Forecasting (WRF) model [*Skamarock et al.*, 2008], the Simulating Waves Nearshore (SWAN) model [*Booij et al.*, 1999], and the Community Sediment Transport Model (CSTM) [*Warner et al.*, 2008]. The Model Coupling Toolkit (MCT) handles the exchange of key atmospheric and oceanic fields between models [*Larson et al.*, 2005]. The COAWST configuration for this study is comprised of WRF and ROMS coupling only.

Specifically, we apply WRF ARW Version 3.1 in this study. WRF ARW (Advanced Research WRF dynamical core, http://www.wrf-model.org) integrates the fully compressible, non-hydrostatic governing equations on a terrain-following vertical coordinate system. It offers sophisticated physics parameterization schemes for handling surface radiation fluxes, boundary layer processes, and precipitation processes. Longwave and shortwave radiation physics are computed by the Rapid Radiative Transfer Model (RRTM) and the Goddard scheme, respectively. The Monin-Obukhov atmospheric surface layer model and the Noah land surface model are used in conjunction with the Mellor-Yamada-Janjic (MYJ) 1.5-order prognostic turbulent kinetic energy (TKE) planetary boundary layer (PBL) scheme. The atmospheric and land surface layer models calculate exchange coefficients and surface fluxes off the land or ocean surface and pass them to the MYJ PBL model every time step. The WRF Single-Moment (WSM) 6-class moisture microphysics scheme represents grid-scale precipitation processes (vapor, cloud, rain, snow, ice, and graupel) and the New Kain-Fritsch cumulus scheme represents sub-grid scale convection and cloud detrainment.

The ROMS ocean circulation model is a free-surface, hydrostatic, primitive equation model used extensively for estuarine, coastal, and basin-scale research applications

(http://www.myroms.org). The ROMS coordinate system is formulated on a horizontal curvilinear Arakawa C-grid with stretched, terrain-following vertical levels. ROMS includes various accurate, high-order numerical schemes for subgrid-scale advection and diffusion. We use the *Mellor-Yamada* [1982] level-2.5 closure scheme to compute vertical turbulent mixing, as well as the quadratic drag formulation for the bottom friction specification.

Fields exchanged in the two-way coupled WRF/ROMS system are wind stress (τ), net heat flux, and sea surface temperature (**Figure 2**). The time steps for WRF and ROMS are 60 and 300 seconds, respectively. During the simulation, wind stress and net heat flux generated by WRF and SST by ROMS are exchanged on each coupling time interval, which is 600 seconds.

2.2 Datasets

Initial and lateral boundary conditions for WRF are obtained from NCEP North American Regional Reanalysis (NARR). NARR reanalysis data are available for the North American region since January 1979 at 3-hourly intervals with 1/3° (32 km) spatial resolution.

Initial and lateral boundary conditions for ROMS are acquired from the Hybrid Coordinate Ocean Model (HYCOM) Navy Coupled Ocean Data Assimilation (NCODA) simulation. The global HYCOM NCODA output is available daily at 1/12° (~10 km) spatial resolution since November 2003. Open boundary conditions (OBCs) were applied at the southern and eastern lateral boundaries (**Figure 3**) to tracers and baroclinic velocity following the method of *Marchesiello et al*. [2001]. Free surface and depth-averaged

velocity boundary conditions were specified using the method of *Flather* [1976] with the external values defined by HYCOM. Tides and rivers were excluded from this ocean model setup since our focus here is on winter-time synoptic scale air-sea interactions.

2.3 Model Setup

We ran the model simulation from 13-31 January 2005, during which time a total of five extratropical cyclones impacted the east coast of the United States. While the COAWST domain encompasses central and eastern North America, the Gulf of Mexico, and the western Atlantic Ocean (**Figure 3**), we focus our analyses over the western Atlantic Ocean centered on Cape Hatteras, NC, to study the 22-23 January 2005 "bomb" ETC which developed along the northeast coast of the United States. The WRF grid is 225 x 236 in the east-west and north-south directions, respectively, with 15 km horizontal resolution and 48 vertical levels. The ROMS grid is 774 x 832 with 5 km horizontal resolution and 18 vertical levels. Since WRF and ROMS are on different grids, the Spherical Coordinate Remapping and Interpolation Package [SCRIP; *Jones*, 1998] program is used to create interpolation weights between different model grids. As such, wind stress and net heat flux from WRF are interpolated to the ROMS model grid and SST from ROMS is interpolated to the WRF model grid for field exchanges.

3. Synoptic Description

An examination of observational time series (**Figure 4**) from National Data Buoy Center (NDBC) buoy 44009 located just off the Delaware coast (**Figure 3**) indicates a period

of weak atmospheric forcing conditions from 1-12 January 2005, which was followed by strong atmospheric forcing conditions from 13-31 January 2005. During the first half of the month, calm, southerly winds prevailed with air temperatures about the same as the ocean temperatures, and low (around zero) sensible and latent heat flux variations. In contrast, the second half of month (13-31 January) was characterized by strong ETCs, sharp drops in air temperature (up to 20 °C) and ocean temperature (up to 5 °C), and large sensible and latent heat fluxes out of the ocean (positive, up to 600 W m^{-2}).

The focus of our dynamical analysis is on the "bomb" ETC that impacted the study area on 22-25 January 2005. At 21Z 22 January, a 1004-mb low formed offshore north of Cape Hatteras (**Figure 5a**). This area of low pressure intensified into a mid-latitude cyclone with upper-level support from a 500-mb trough over the eastern U.S. (not shown). Over the first 12 hours, its central pressure dropped rapidly by 16 mb as the cyclone tracked northeastward, and a strong cold front oriented northeast to southwest had swept over the MAB and SAB (**Figure 5b**). The cyclone continued deepening to 980 mb after 24 hours, meeting *Sanders and Gyakum's* [1980] criteria for "bomb" cyclones. Enhanced northwesterly winds persisted over the MAB for two days as the ETC moved through the study region (**Figure 5c**). The near-freezing air temperatures and high wind speeds during this storm (between the dashed lines on **Figure 4**) provided strong atmospheric forcing to the underlying ocean.

4. Coupled Model Performance

The performance of our coupled model simulation was gauged against the hourly time series of surface winds, sea level pressure (SLP), air temperature, and SST measured by NDBC buoys 44009, 41004, and 41001, as well as ocean temperature measured along the Rutgers University glider transect (http://marine.rutgers.edu/mrs/projects/oceanrobots.htm) across the northern MAB shelf (see their locations in **Figure 3**). NDBC buoy measurements are located in three distinct ocean regimes: the cool shelf water in the MAB (buoy 44009), the seaward side of the Gulf Stream offshore of Cape Hatteras (buoy 41001), and the warm mid-shelf water in the SAB (buoy 41004). Buoy data were 36-hour low-pass filtered and sub-sampled every three hours to be concurrent with model output over the time period 13-31 January 2005. In-situ observations were directly compared to the corresponding value at the closest model grid point or model transect. Each model-data wind time series comparison was quantified by a vector correlation coefficient, vector orientation difference, and vector regression coefficient (r, Θ, and Reg, respectively). Sea level pressure, air temperature, and SST comparisons were quantified by their correlation coefficient (r) and root mean square error (RMS error).

The wind time series comparison (**Figure 6**) shows excellent correspondence between observation and model (correlation coefficients greater than 0.84). In particular, the coupled model successfully captures the high wind speeds (regressions ranging from 0.99-1.03) and the sharp changes in wind direction (mean offsets only about 5° in the clockwise direction) with each passing ETC.

Modeled SLP also matches well with buoy-measured SLP (**Figure 7**). The correlation coefficients are greater than 0.98 with mean offsets of about 1.5 mb. Likewise, favorable agreement is found in the air temperature comparison. The coupled simulation reproduces the temporal variability in surface air temperature well, with correlation coefficients greater than 0.96 (**Figure 8**). We note that the model overestimates (by up to about 2.7 °C) air temperature during ETCs. Such "cold bias" in the observations is likely a result of enhanced evaporation due to storm-induced wave breaking [*J. Bane*, personal communication], a process that is not accounted for in our coupled air-sea model simulation.

Sea surface temperature comparisons (**Figure 9**) are reasonable as well except at buoy 41004. The differences are due to a number of factors including the spatial offsets between the buoy measurement and the closest model grid point and the difference between the bulk ocean temperature measured 1-m below the surface by the buoy and the temperature of the top vertical layer simulated by the model. For 41004 in particular, the lateral movements of the Gulf Stream on the SAB shelf from 16 to 22 January are not well captured by the 5-km resolution ocean model, and for the remainder of January, the modeled surface temperatures lag behind its observed counterpart, resulting in a low correlation at this location. Temperature time series are highly correlated (>0.96) with less than 0.6 °C bias at the other two stations (44009 and 41001).

The subsurface temperature comparison between the glider observation and the coupled simulation on 14 January 2005 is very good (**Figure 10**). The ocean model accurately reproduces the well-mixed shelf waters, the horizontal temperature gradient

(increasing from 7 to 9 °C in the offshore direction), and most of the small-scale horizontal temperature structures.

Based on these favorable comparisons to in-situ observations, we conclude that our two-way coupled model simulation produced realistic oceanic and atmospheric conditions during the ETC outbreak in January 2005, lending confidence that the dynamical analysis described below is couched in a realistic air-sea environment.

5. Coupled Model Analysis

5.1 Atmosphere-Ocean Feedbacks

To illustrate the air-sea interactions during the passage of a "bomb" extratropical cyclone, we examine vertical profiles of the upper ocean and the lower atmosphere across three transects off the U.S. east coast. Specifically, transect T1 spans the northern MAB shelf and shelfbreak, T2 spans the SAB shelf and the Gulf Stream off Cape Hatteras, and T3 spans the SAB shelf and the Gulf Stream off South Carolina (transect locations are shown in **Figure 3**). Each transect is roughly 250 km long and oriented perpendicular to the coastline. Along each transect, the air temperature and normalized vertical winds (showing wind direction only) from sea level to 800 mb (top panel), the thermal structure of the upper 100 m of the ocean (bottom panel), and the along-transect SST profile and the change in SST during the storm passage (middle panel) are presented (**Figures 11-13**). The change in SST (ΔSST) is calculated as the difference between the SST at a given time and the SST on 00Z 22 January. An animation showing the vertical profiles at three-hourly intervals from 22-25 January 2005 can be viewed online at

http://omglnx7.meas.ncsu.edu/jsnelson/profile_anim/atm2ocn.htm. We also present four spatial maps of modeled surface air temperature, SLP contours, and synoptic winds (**Figure 14**) showing the atmospheric conditions one day prior to the storm (00Z 22 January), during the ETC formation (00Z 23 January), at the onset of the cold air outbreak following the frontal passage (09Z 23 January), and at the end of the cold air outbreak (00Z January 25).

At 00Z 22 January, northerly winds prevail over the western Atlantic Ocean due to the clockwise circulation around a synoptic high pressure system located on the northeastern U.S. coastline (**Figure 14a**). Along the northernmost transect (T1), the water column is well-mixed with water temperatures of ~8 °C near the coast increasing to ~14 °C beyond the MAB shelfbreak (**Figure 11a**). The air temperatures throughout the MABL are below freezing along T1 with slightly warmer near-surface air temperatures over the shelfbreak waters. Off Cape Hatteras, warm (23 °C) Gulf Stream waters are positioned 40 km from the shoreward end of T2, separating slightly cooler waters (both ~20 °C) over the well-mixed SAB shelf and Sargasso Sea (**Figure 12a**). The Gulf Stream is farther offshore and slightly warmer at T3 than at T2 (**Figure 13a**). Surface air temperatures are ~10 °C cooler near the coast than offshore as mesoscale atmospheric circulations over the Gulf Stream heat the MABL from the surface to 900 mb (**Figures 12-13a**).

Over the next 24 hours, the high pressure system moves away from the study region and the low forms off Cape Hatteras. By 00Z 23 January, the center of the low is positioned over T1 while T2 and T3 are in the warm sector of the storm and the prevailing flow over the Atlantic Ocean comes out of the south-southwest, accelerating toward the low pressure center (**Figure 14b**). At this time, the inflow of warm air from the south converges ahead of

the front and destabilizes the atmosphere, generating upward motions and warming the MABL by 10-15 °C (**Figure 11-13b**). The upward winds and the rapid MABL heating are important for cyclone intensification over the next several hours. The ocean response is small (<1 °C ocean temperature decrease at each location) during this early stage of the ETC development (**Figure 11-13b**).

The cold air outbreak begins at 09Z 23 January when a cold, dry air mass sweeps offshore behind the front (**Figure 11-14c**) and lasts until 00Z 25 January. Most of the ocean cooling occurs during these two days (**Figures 11-13d**). Storm enhanced winds and prolonged contact with cold, dry air (i.e. ocean-to-atmosphere sensible and latent heat fluxes) caused the MAB shelf waters and the Gulf Stream to cool up to 2 °C, consistent with the magnitude of the SST decrease observed by *Bane and Osgood* [1989] and *Xue et al*. [1995]. By 00Z 25 January, a ridge of high pressure in the southeastern U.S. (**Figure 14d**) dominates the synoptic atmospheric conditions and the MABL has basically restored to the pre-storm condition.

5.2 Oceanic Heat Budget

To identify the processes resulting in a ~2 °C temperature drop in the upper 100 m of the ocean after the "bomb" ETC passage, we quantify the ocean heat budget along T1, T2, and T3. Temperature changes in the ocean are governed by the thermodynamic equation given by:

$$\frac{\partial T}{\partial t} + \left[u\frac{\partial T}{\partial x} + v\frac{\partial T}{\partial y} + w\frac{\partial T}{\partial z} \right] = \frac{\partial}{\partial z}\left(K\frac{\partial T}{\partial z}\right) + \frac{\partial}{\partial x}\left(A\frac{\partial T}{\partial x}\right) + \frac{\partial}{\partial y}\left(A\frac{\partial T}{\partial y}\right) \qquad (1)$$

where *u*, *v*, and *w* are the cross-shore (*x*-direction), alongshore (*y*-direction), and vertical (*z*-direction) velocity components, *T* is ocean temperature, *t* is time, *K* is the vertical eddy thermal diffusivity, and *A* is the horizontal eddy viscosity. The time rate of temperature change ($\frac{\partial T}{\partial t}$) is the result of horizontal and vertical advection (bracketed terms on the left hand side) and horizontal and vertical diffusion (terms on the right hand side). We note the horizontal diffusion is negligible (not shown), but vertical diffusion can be quite large during a winter storm [*Xue et al.*, 1995].

We diagnose the heat budget along three sections where the lateral boundaries are defined as the onshore and offshore ends of each transect, the top boundary is the sea surface, and the bottom boundary is set to a depth of 100 m. Depth-integrating Equation 1 for the upper 100-m of the water column along each transect for the three-day storm period (22-25 January 2005), in conjunction with the boundary conditions for ocean temperature, yields the following heat balance equation:

$$\Delta H = H_{adv} + H_{flux} \qquad (2)$$

so that $\Delta H = \rho C_p \int_{-100}^{\eta} \frac{\partial T}{\partial t} dz$ is the local rate of change in heat content of the section resulting from (a) vertical and horizontal heat advection in the water column $H_{adv} = \rho C_p \int_{-100}^{\eta} (-u\frac{\partial T}{\partial x} - v\frac{\partial T}{\partial y} - w\frac{\partial T}{\partial z})dz$ and (b) vertical heat diffusion $H_{flux} = Q - (K\frac{\partial T}{\partial z})_{z=-100m}$ where Q is the net surface heat flux (the sum of sensible heat,

latent heat, shortwave radiation, and longwave radiation) and $(K\frac{\partial T}{\partial z})_{z=-100m}$ is the heat diffusion at 100-m, and ρ and C_p are seawater density (taken as 1025 kg/m^3) and specific heat (3990 J/kg·K), respectively. The vertical diffusion flux across 100-m (not shown) is very small, being only about -5 W m^{-2} on average, and is thus ignored in the analysis below.

Heat budget time series along all three transects (left column of **Figure 15**) reveal several common features: (1) the net surface heat flux (H_{flux}) are all negative, indicating that the ocean is losing heat during the three-day period; (2) large, rapid cooling occurs around the mid-day of 23 January, followed by a steady warming trend right after it; and (3) the high frequency variability of ocean heat change is determined by ocean advection.

The temporal mean (three-day average) heat budget (right column of **Figure 15**) provides a valuable insight on regional contrast. At T1, both H_{flux} and H_{adv} contribute to the ocean cooling, roughly at 80% and 20% of ΔH (-600 W m^{-2}), respectively. A major portion of section T1 is located on the shallow shelf where significant water temperature deceases are seen (**Figure 11**). Shallow water temperature changes at this section thus result primarily from air-sea heat flux exchange during the storm.

Both T2 and T3 run through the Gulf Stream and display a different heat balance. Because of the persistent Gulf Stream transport of warmer waters from the south, the warming effect of ocean advection and the cooling effect of surface heat flux counteract each other, resulting in a weaker cooling tendency. This is especially true at T2 (off Cape Hatteras), where the ocean advection associated with the Gulf Stream is the strongest. Nevertheless, the large ocean-to-atmosphere heat flux loss during this "bomb" ETC remains

the dominant process for the upper ocean temperature budget. At all three transects, the cooling tendency due to H_{flux} is 2-4 times larger than the warming tendency due to H_{adv}.

6. Summary and Conclusions

We utilized a new ocean (ROMS)-atmosphere (WRF) coupled modeling system to simulate the winter extratropical storm outbreak in January 2005. During the simulation, two-way coupling was achieved by exchanging the wind stress and net heat flux fields produced by the WRF model and the SST field produced by the ROMS model every 10 minutes. In general, the coupled simulation accurately reproduced atmospheric and oceanic conditions. Detailed atmosphere-ocean feedbacks were examined for a three-day storm period (22-25 January 2005), when a "bomb" ETC formed near Cape Hatteras and intensified rapidly on its track across the northwest Atlantic Ocean. Our model diagnostics show upward air motions triggered by surface wind convergence ahead of the cold front and MABL heating support the storm's rapid intensification off the U.S. east coast. Furthermore the heat loss from the ocean, together with locally enhanced winds, can cool the Gulf Stream and shelf water by up to 2 °C. From the heat budget perspective, on the shallow MAB shelf (e.g., T1), both oceanic heat loss and oceanic advection contribute to the cooling, whereas in regions near the Gulf Stream (e.g., T2 and T3), the cooling effect due to ocean heat loss counteracts the warming effect of Gulf Stream advection.

To demonstrate the importance of air-sea coupling during winter extratropical cyclones we also performed two other model sensitivity experiments, including an *uncoupled run*: WRF-only simulation with a time-invariant SST taken from Real Time Global SST

(RTG-SST, http://polar.ncep.noaa.gov/sst/) analysis on 00Z 13 January 2005; and a *one-way coupled run*: WRF-only simulation with a low-resolution SST linearly interpolated every three hours from daily RTG-SST data from 13-31 January 2005. We note that employing a static SST condition as in the *uncoupled run* or a low-resolution, interpolated SST field as in the *one-way coupled run* represents a standard approach for handling SST (thus ocean feedback) in short (days to weeks) atmospheric model forecasts. Time series comparisons (not shown) indicate that the observed variability in surface winds, SLP, and surface air temperature can be resolved by the *uncoupled* and *one-way coupled runs* for this fast-moving "bomb" ETC, but the two-way coupled simulation (the *control run* as presented in this study) produced the best skill (lowest errors) in predicting surface wind, air temperature, and ocean temperature. Because ocean feedback will become more important for slow-moving storms, we expect the advantage of a two-way coupled simulation can stand out even more clearly for such events. Through a more detailed theoretical analysis, *Nelson and He* [submitted] show that synoptic-scale surface wind convergence is inversely proportional to the Laplacian of ocean surface temperature. Such two-way air-sea dynamic coupling can be derived from the rather simple, linear Ekman and Geostrophic MABL model described in *Minobe et al*. [2008] and *Lindzen and Nigam* [1987]. Not surprisingly, only the two-way coupled simulation (the *control run*) can arrive at the best agreement with this theoretical basis on the relationship between surface wind convergence and Laplacian of SST. We conclude that in order to improve ETC predictions and regional coastal wind and wind energy potential assessment in general, air-sea interactions affecting momentum and buoyancy flux exchanges have to be accurately accounted for in a coupled atmosphere-ocean modeling framework.

Acknowledgements

We are grateful to the funding support provided by NSF and ONR through grants OCE-0927470 and N00014-06-1-0739, respectively. We thank Dr. J. Warner of USGS for productive collaboration and leading the effort in developing and testing the COAWST modeling system, and Dr. J. Bane of UNC for scientific guidance and many enlightening discussions. Z. Yao's assistance in setting up the ocean model is appreciated. Results and analyses presented here are part of J. Nelson master's thesis research at North Carolina State University.

REFERENCES

Bane, J. M., and K. E. Osgood (1989), Wintertime air-sea interaction processes across the Gulf Stream, *J. Geophys. Res.*, *94*, 10755-10772.

Booij, N., R. C. Ris, and L. H. Holthuijsen (1999), A third-generation wave model for coastal regions. Part I: Model description and validation. *J. Geophys. Res.*, *104*, 7649–7666.

Colucci, S. J. (1976), Winter cyclone frequencies over the eastern United States and adjacent western Atlantic, 1964-1973, *Bull. Am. Meteor. Soc.*, *57*(5), 548-553.

DeGaetano, A. T. (2008), Predictability of seasonal east coast winter storm surge impacts with application to New York's Long Island, *Meteor. Appl.*, *15*, 231-242.

Dirks, R. A., J. P. Kuettner, and J. A. Moore (1988), Genesis of Atlantic Lows Experiment (GALE): An overview, *Bull. Am. Meteor. Soc.*, *69*(2), 148-160.

Flather, R. A. (1976), A tidal model of the north-west European continental shelf. *Mem. Soc. R. Sci. Liege*, *6*, 141-164.

Hirsch, M. E., A. T. DeGaetano, and S. J. Colucci (2001), An east coast winter storm climatology, *J. Climate, 14*, 882-899.

Jones, P. W. (1998), A user's guide for SCRIP: A Spherical Coordinate Remapping and Interpolation Package. Los Alamos National Laboratory. WWW page: http://climate.lanl.gov/Software/SCRIP/.

Larson J., R. Jacob, and E. Ong (2005), The Model Coupling Toolkit: A new FORTRAN90 toolkit for building multiphysics parallel coupled models. *Int. J. High Perform. C.*, *19*, 277-292.

Lindzen R. S., and S. Nigam (1987), On the role of sea surface temperature gradients in forcing low-level winds and convergence in the tropics, *J. Atmos. Sci.*, *44*(7), 2418-2436.

Marchesiello, P., J. C. McWilliams, and A. Shchepetkin (2001), Open boundary conditions for long-term integration of regional ocean models, *Ocean Modell.*, *3*, 1-20.

Mellor, L. G., and T. Yamada (1982), Development of a turbulence closure model for geophysical fluid problems, *Geophys. Space Phys.*, *20*, 851-875.

Miles, T. and R. He (2010), Seasonal surface ocean temporal and spatial variability of the South Atlantic Bight: Revisiting with MODIS SST and Chl-a imagery, *Cont. Shelf Res.*, *30*, 1951-1962.

Minobe, S., A. Kuwano-Yoshida, N. Komori, S.-P. Xie, and R. J. Small (2008), Influence of the Gulf Stream on the troposphere, *Nature*, *452*, 206-210, doi:10.1038/nature06690.

Nelson, J. S., and R. He, submitted, Effect of the Gulf Stream on winter extratropical cyclone outbreaks, *Atmos. Sci. Lett.*

Reddy, N. C., and S. Raman (1994), Observations of a mesoscale circulation over the Gulf Stream region, *Global Atmos. Ocean Syst.*, *2*, 21-39.

Sanders, F., and J. R. Gyakum (1980), Synoptic-dynamic climatology of the "bomb", *Mon. Weather Rev.*, *108*, 1589-1606.

Shchepetkin, A. F., and J. C. McWilliams (2005), The Regional Ocean Modeling System: A split-explicit, free-surface, topography-following coordinates ocean model, *Ocean Modell.*, *9*, 347–404.

Skamarock, W. C., J. B. Klemp, J. Dudhia, D. O. Gill, D. M. Barker, M. G. Duda, X.-Y. Huang, W. Wang, and J. G. Powers (2008), A description of the Advanced Research WRF Version 3, Technical note, National Center for Atmospheric Research, TN-475+STR, WWW page: http://www.mmm.ucar.edu/wrf/users/docs/arw_v3.pdf.

Small, R. J., S. P. deSzoeke, S. P. Xie, L. O'Neill, H. Seo, Q. Song, P. Cornillon, M. Spall, and S. Minobe (2008), Air-sea interactions over ocean fronts and eddies, *Dyn. Atmos. Oceans*, *45*, 274-319.

Warner, J. C., B. Armstrong, R. He, and J. B. Zambon (2010), Development of a Coupled-Ocean-Atmosphere-Wave-Sediment-Transport (COAWST) modeling system, *Ocean Modell.*, *35*, 230-244, doi:10.1016/j.ocemod.2010.07.010.

Warner, J. C., C. R. Sherwood, R. P. Signell, C. K. Harris, and H. G. Arango (2008), Development of a three-dimensional, regional, coupled wave, current, and sediment-transport model. *Comput. Geosci.*, *34*, 1284-1306, doi:10.1016/j.cageo.2008.02.012.

Wayland, R. J., and S. Raman (1994), Structure of the marine atmospheric boundary layer during two cold air oubreaks of varying intensities: GALE 1986, *Bound.-Layer Meteor.*, *71*, 43-66.

Xue, H., J. M. Bane, and L. M. Goodman (1995), Modification of the Gulf Stream through strong air-sea interactions in winter: Observations and numerical simulations, *J. Phys. Oceanogr.*, *25*, 533-557.

Zishka, K. M., and P. J. Smith (1980), The climatology of cyclones and anticyclones over North America and surrounding ocean environs for January and July, 1950-77, *Mon. Weather Rev.*, *108*(4), 387-401.

FIGURES

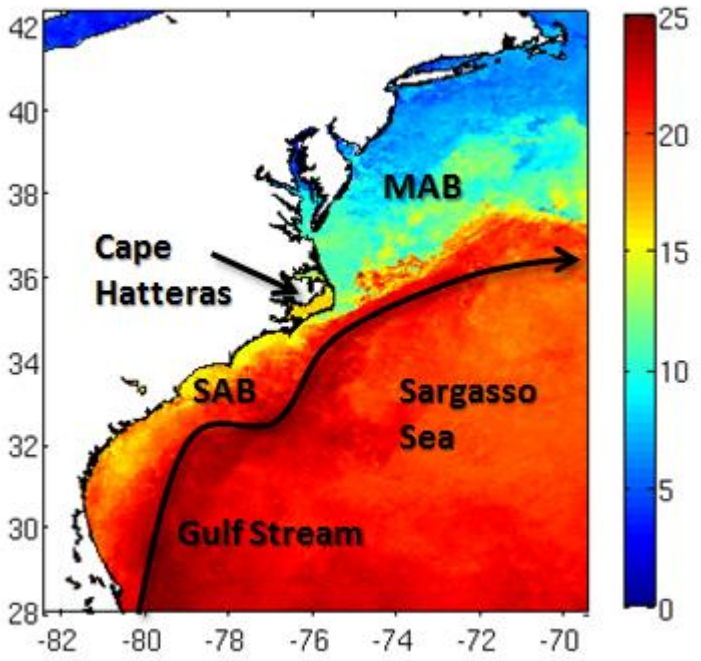

Figure 1. Satellite SST in the western Atlantic Ocean valid on 13 January 2005. Missing SST due to cloud cover was reconstructed using the DINEOF method [*Miles and He*, 2010]. MAB and SAB are the Middle Atlantic Bight and South Atlantic Bight, respectively.

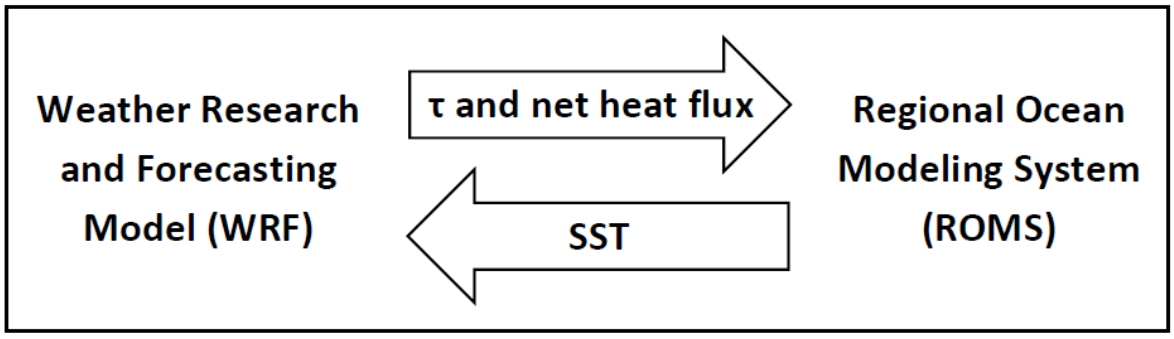

Figure 2. A diagram showing the fields exchanged in the two-way coupled WRF/ROMS model simulation.

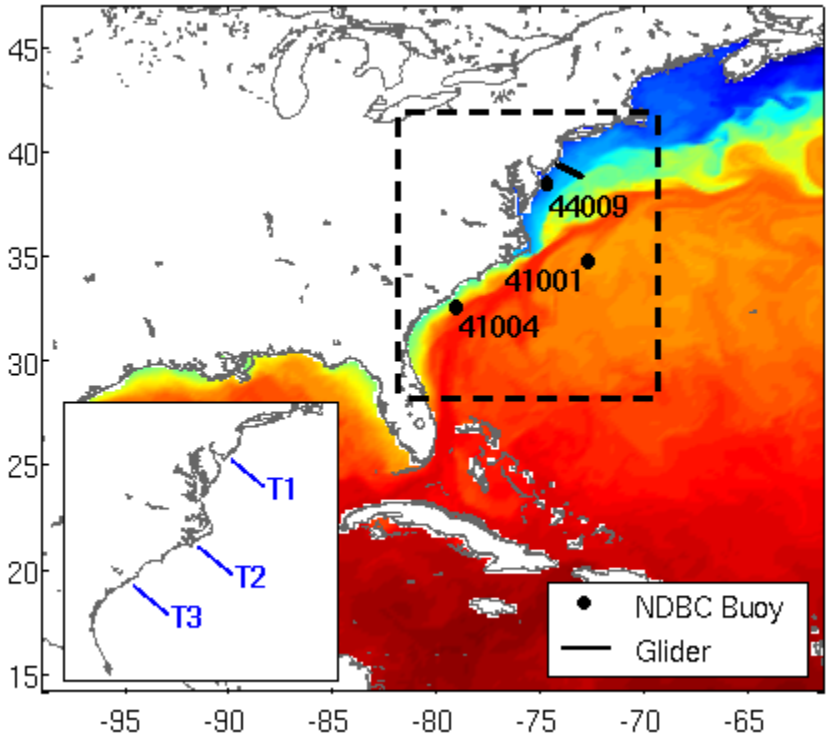

Figure 3. The COAWST model domain (solid box encompassing central and eastern North America, the Gulf of Mexico, and the western Atlantic Ocean) and focus region (dashed box). Also shown are the locations of three NDBC buoys, the Rutgers University glider transect, and three cross-shelf transects (T1-T3) along which vertical wind, air temperature, and ocean temperature structures are diagnosed.

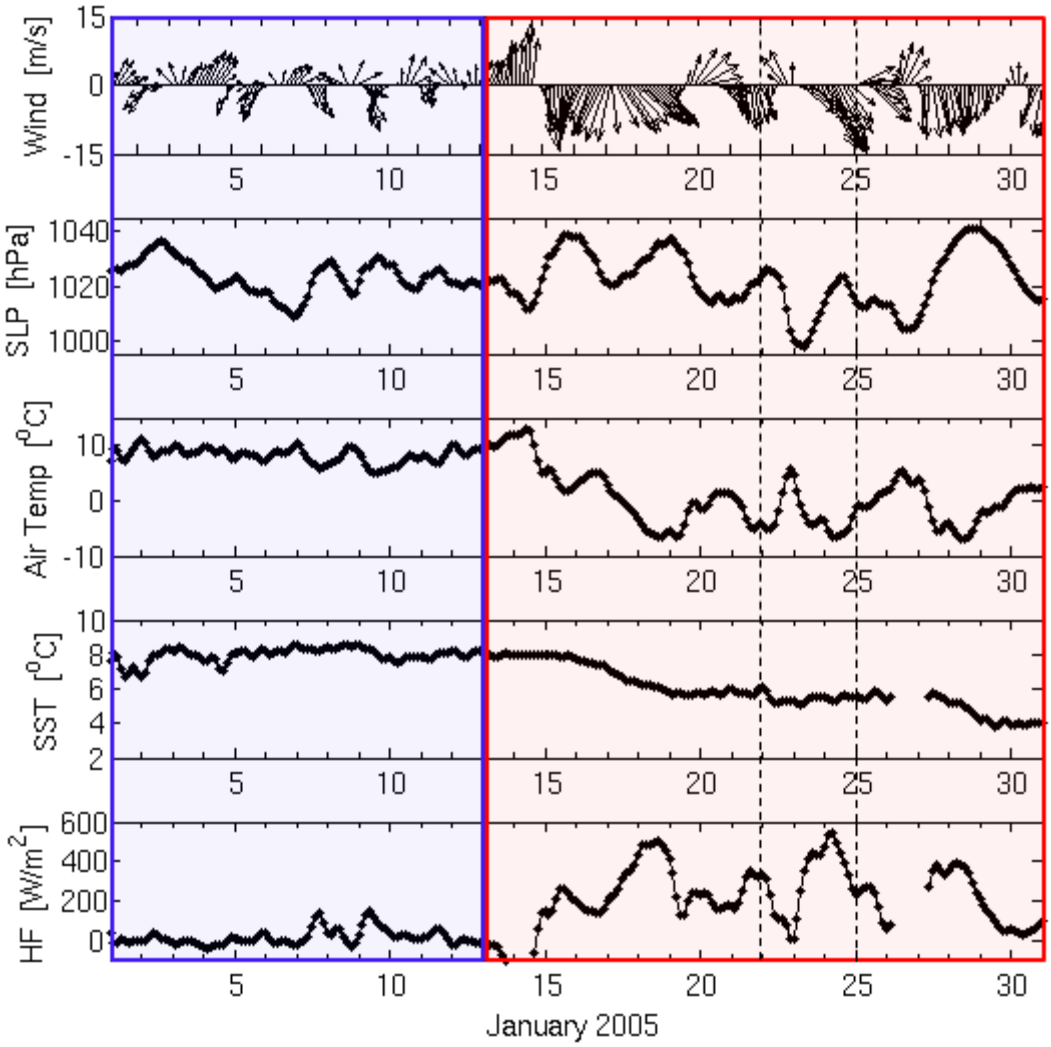

Figure 4. Time series of observed winds, sea level pressure (SLP), air temperature, SST, and total heat flux (HF) at buoy 44009 in January 2005. The first half of the month (1-12 January; blue) is characterized by relatively calm conditions and followed by a period of strong atmospheric forcing condition (13-31 January; red) associated with the passage of five ETCs. The effects of the 22-23 January "bomb" ETC are indicated between the black dashed lines.

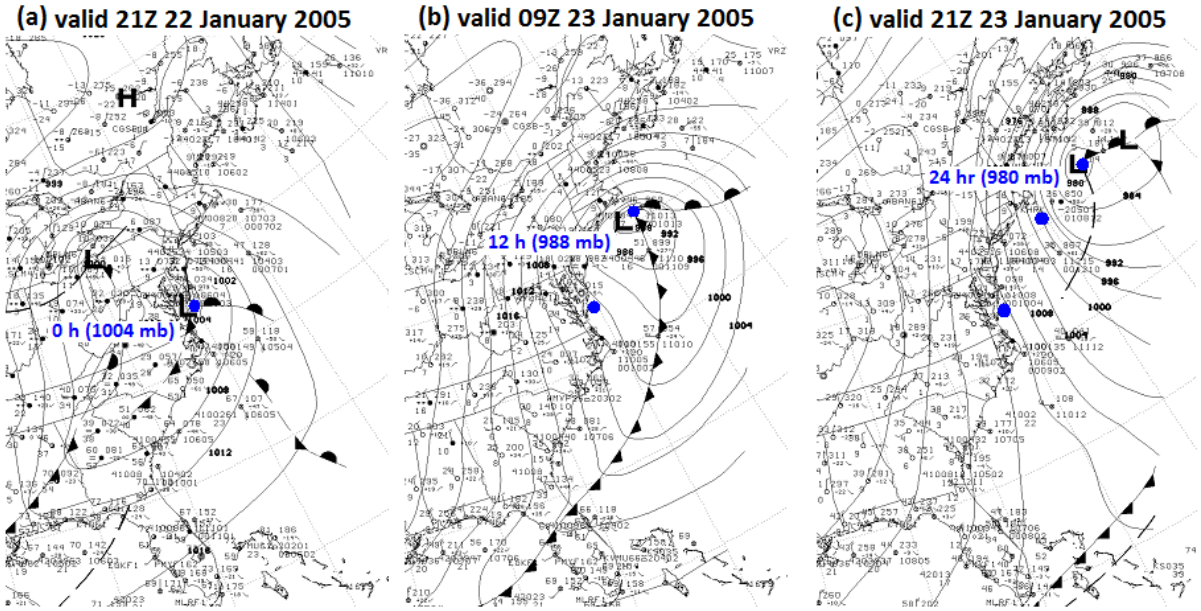

Figure 5. National Weather Service (NWS) surface analysis charts valid at (a) 21Z 22 January 2005, (b) 09Z 23 January 2005, and (c) 21Z 23 January 2005.

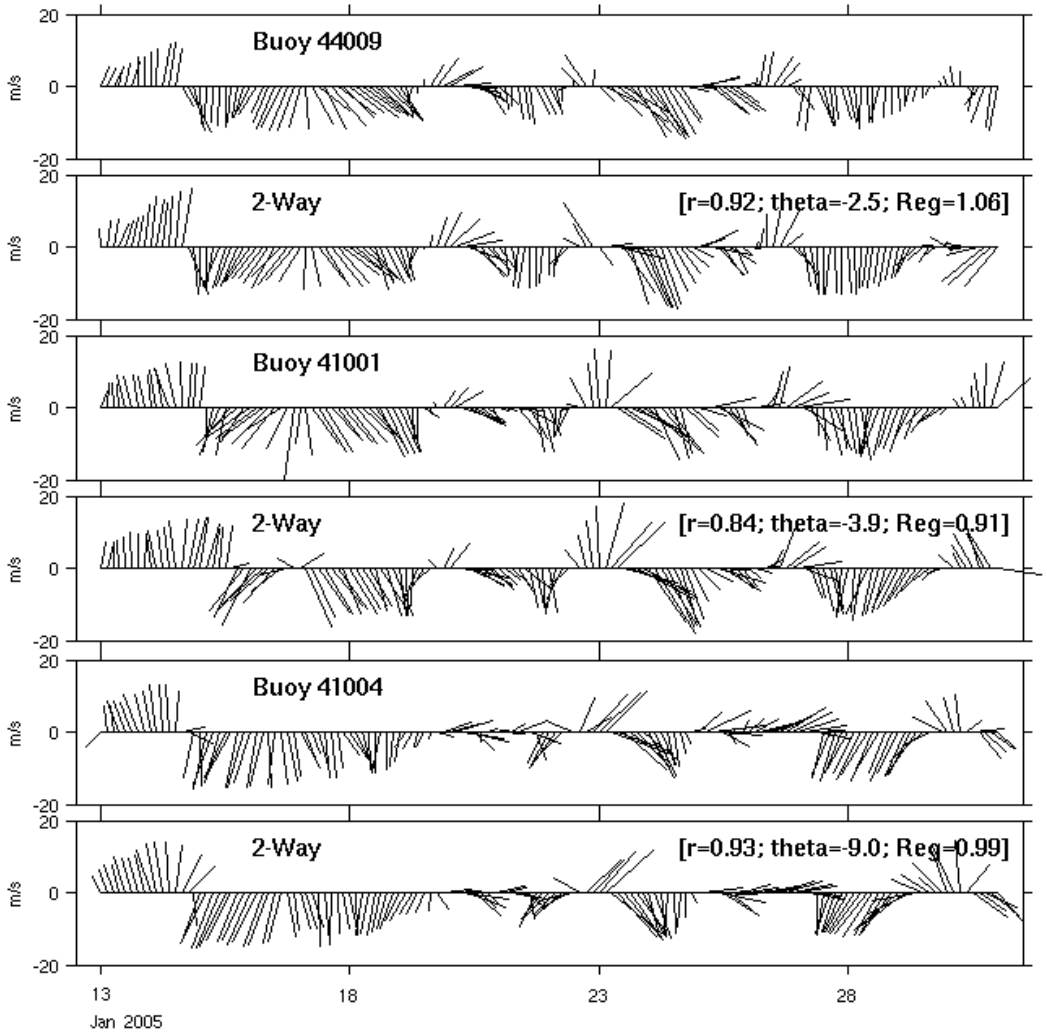

Figure 6. Wind time series comparison. The complex correlation (r, Θ) and magnitude regression coefficient (Reg) between buoy-measured and 2-way coupled model simulated wind time series are shown.

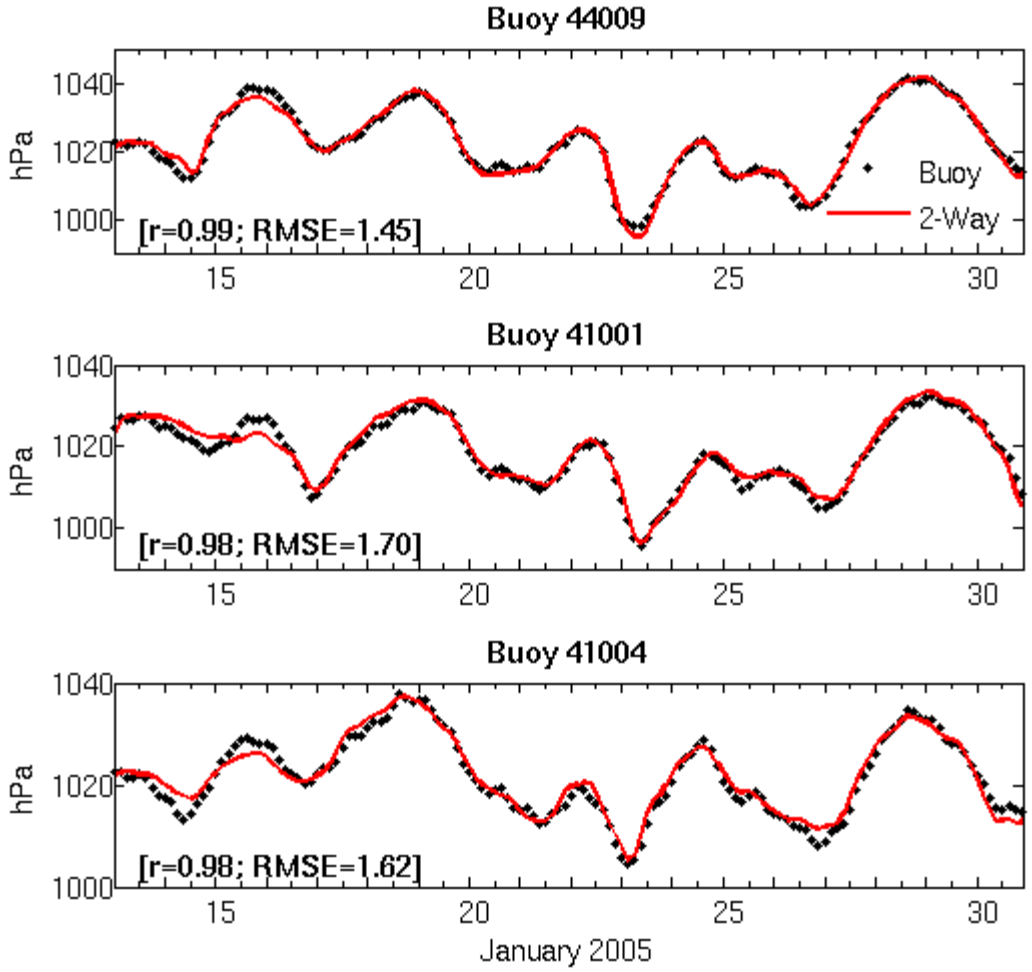

Figure 7. Comparison between buoy observed (black) and model simulated (red) sea level pressure time series. Also shown are their correlation coefficient and RMS error in [mb].

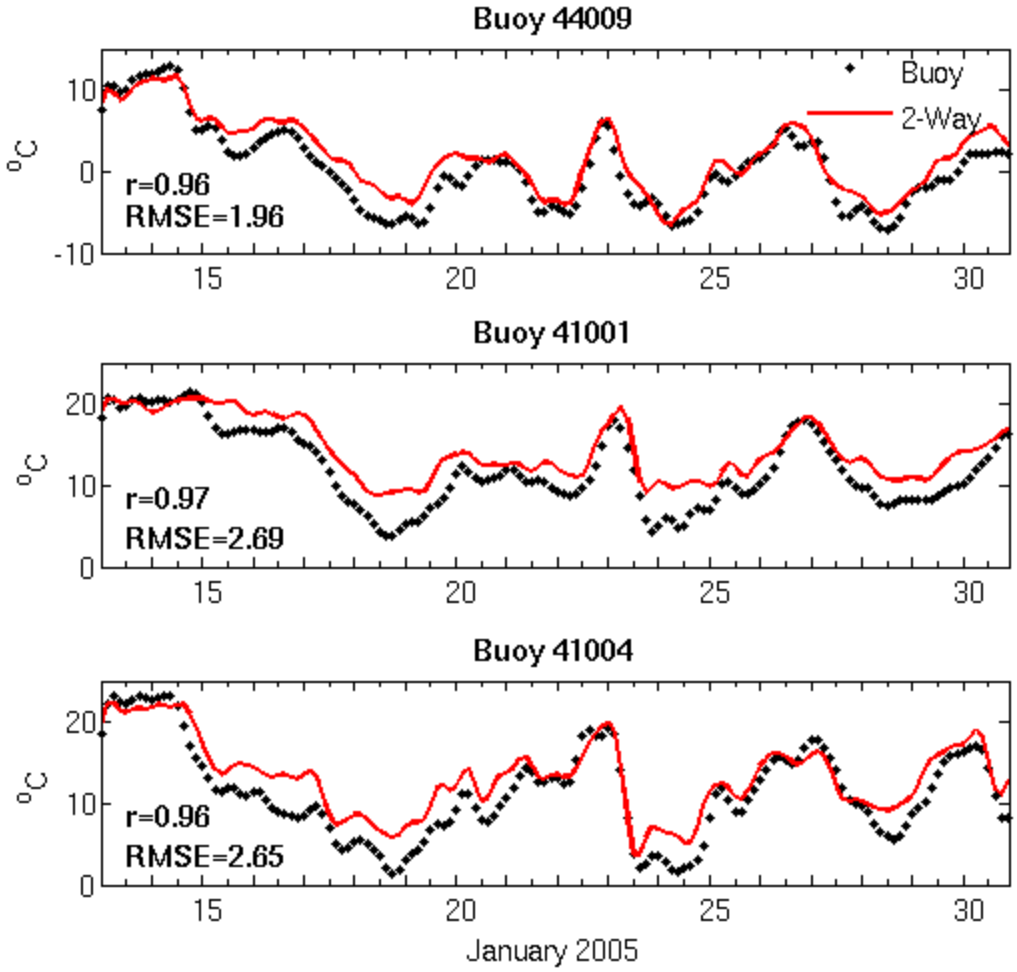

Figure 8. Comparison between buoy observed (black) and model simulated (red) surface air temperature time series. Also shown are their correlation coefficient and RMS error in [°C].

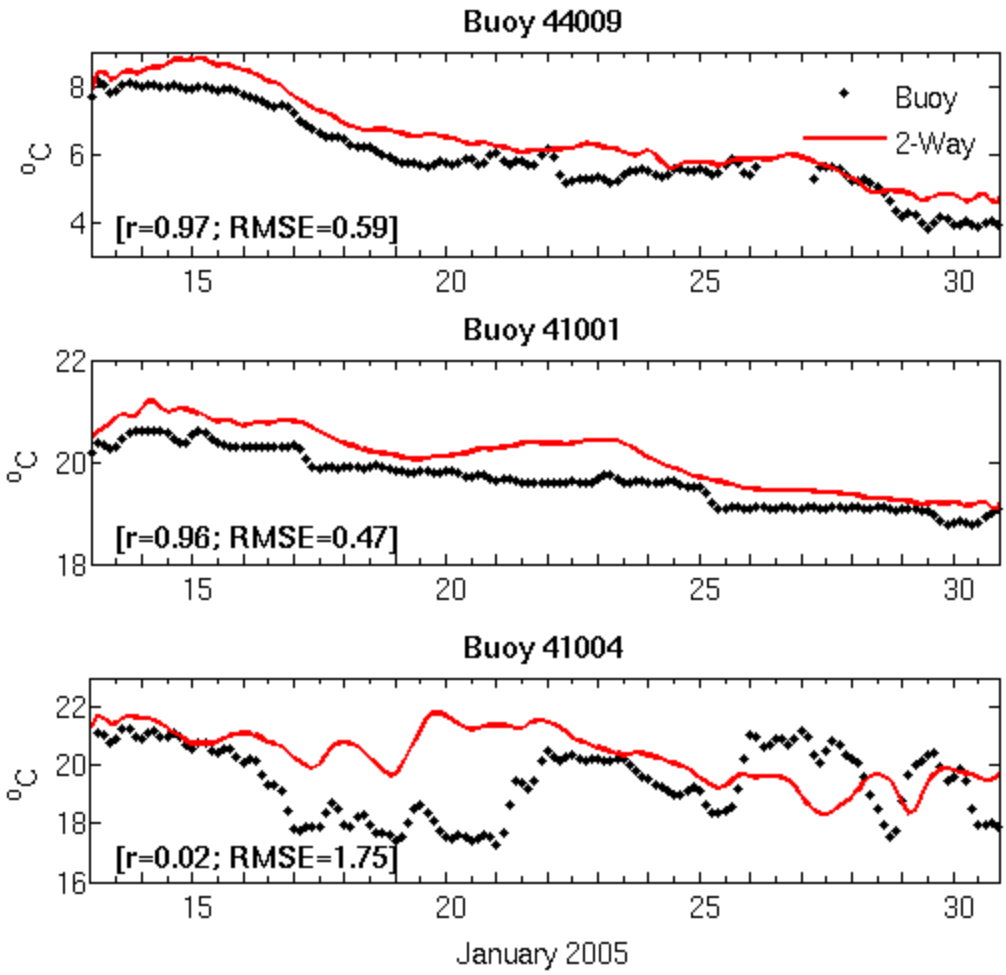

Figure 9. Comparison between buoy observed (black) and model simulated (red) sea surface temperature time series. Also shown are their correlation coefficient and RMS error in [°C].

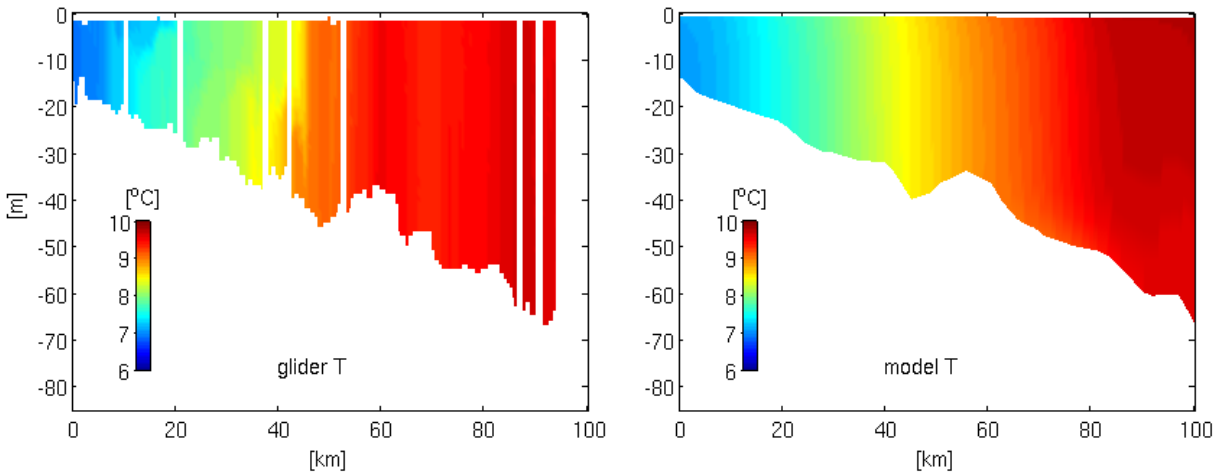

Figure 10. Comparison between glider observed and model simulated cross-shelf ocean temperature structure along the Rutgers University glider transect (see location in Figure 3) on 14 January 2005.

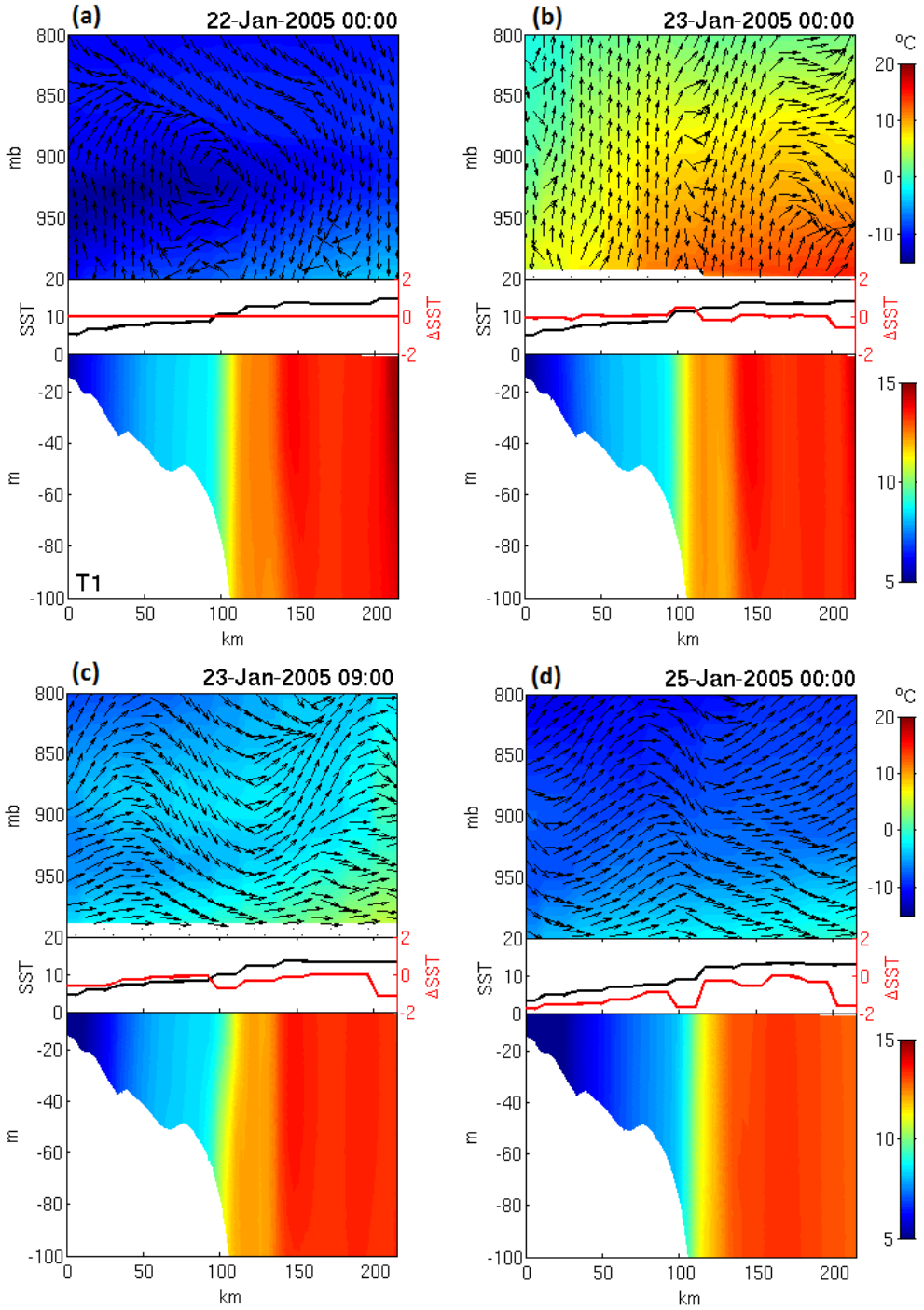

Figure 11. Snapshots of vertical temperature structures of the lower atmosphere (sea level to 800 mb) and upper ocean (sea level to -100 m) along T1. Also shown are the corresponding cross-shelf sea surface temperature (SST) distribution and its anomaly relative to SST at 00Z 22 January 2005 (ΔSST).

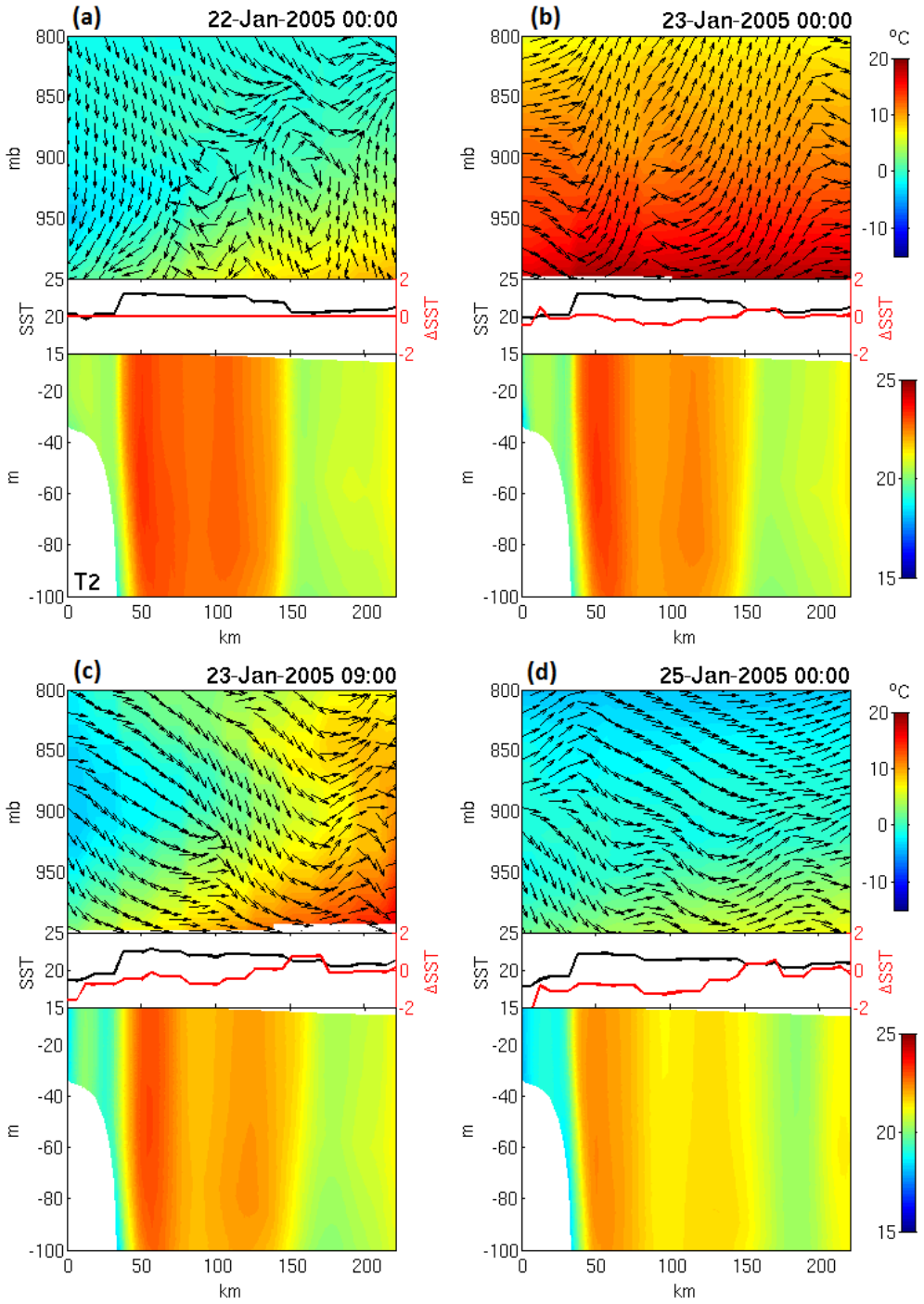

Figure 12. Same as Figure 11, but for T2.

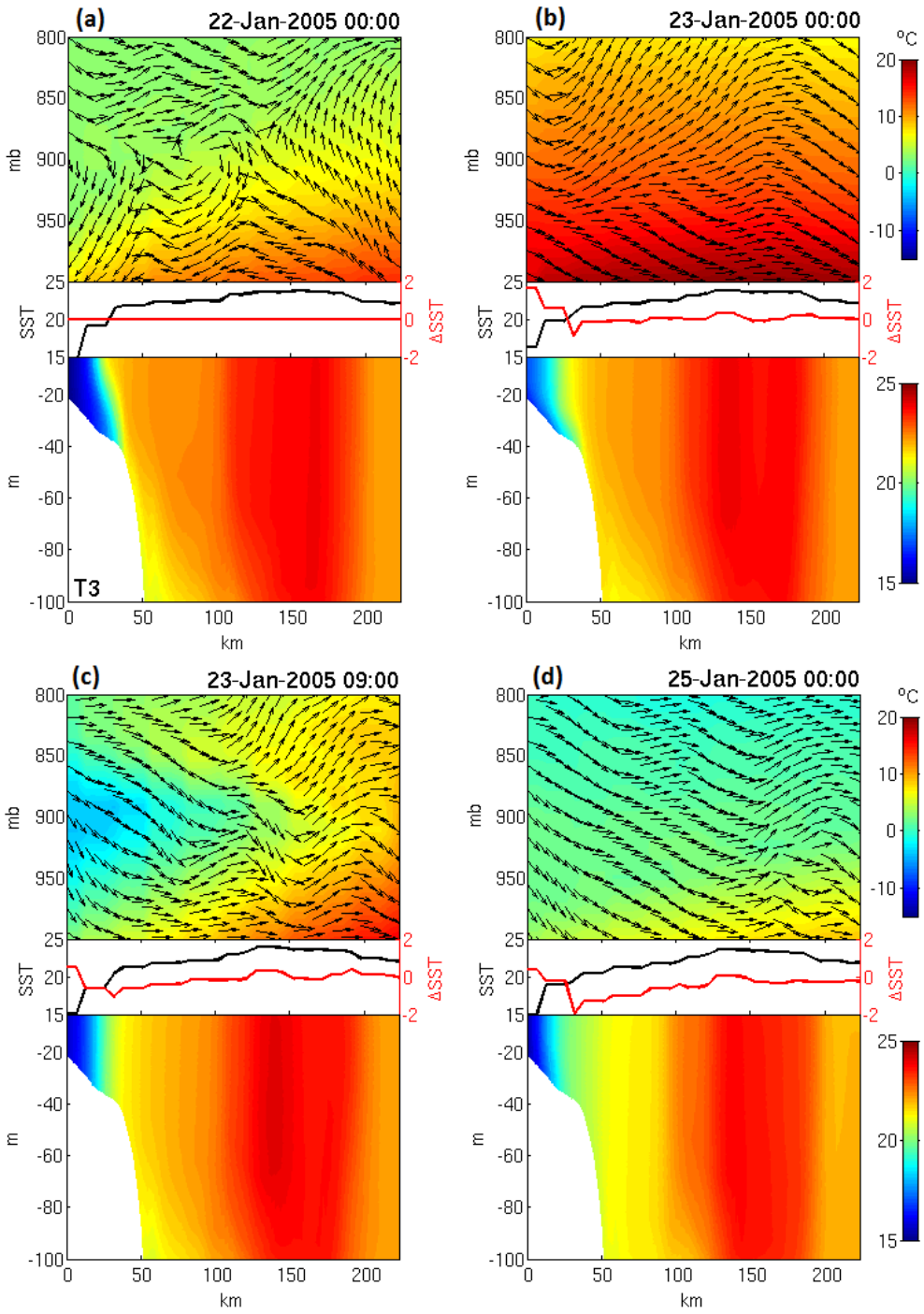

Figure 13. Same as Figure 11, but for T3.

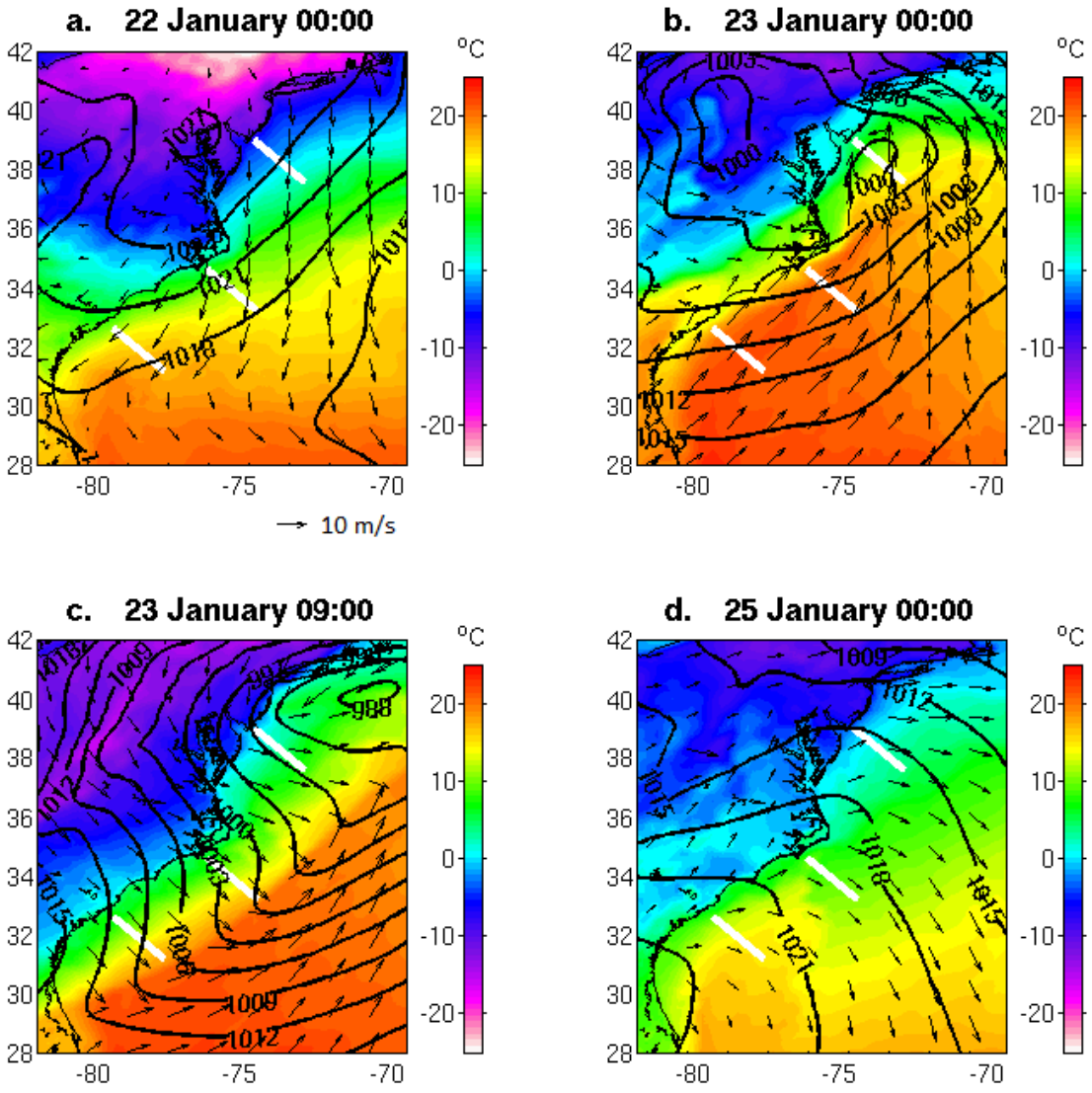

Figure 14. Simulated surface air temperature (shaded), sea level pressure (contours; 3 mb interval), wind vectors, and transect locations (white; T1 to the north, T2 in the middle, and T3 to the south).

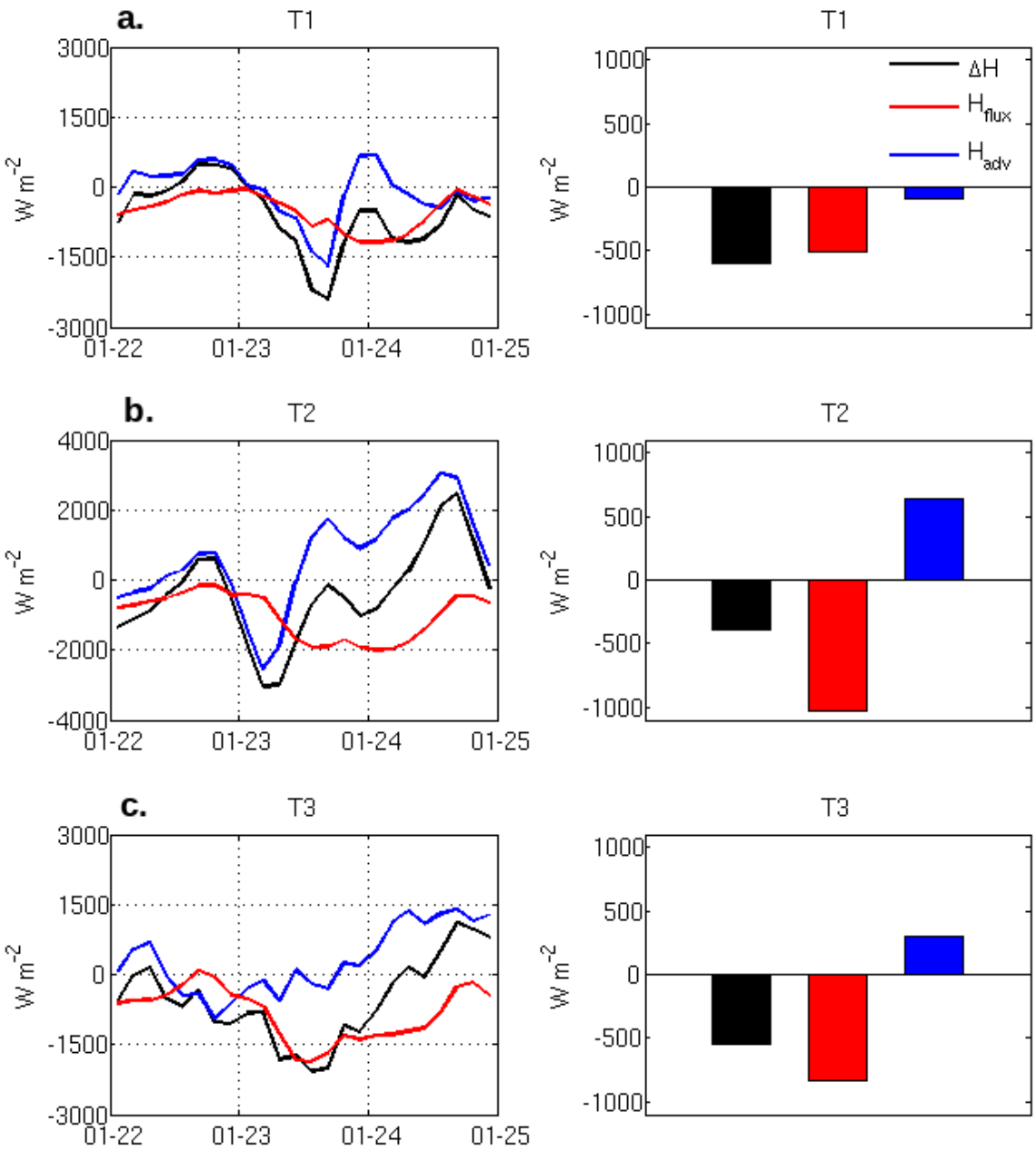

Figure 15. Upper (100-m) ocean heat budget diagnosis at transects T1-3 during the period of the "bomb" ETC (22-25 January). The left column shows the time series of the local rate of heat change ΔH, the net surface heat flux H_{flux}, and the net heat advection H_{adv} averaged over each cross-shelf transect and their corresponding three-day mean values are shown in bar plot format in the right column.

CHAPTER 3

Effect of the Gulf Stream on Winter Extratropical Cyclone Outbreaks

Jill S. Nelson and Ruoying He

Dept. of Marine, Earth, and Atmospheric Sciences

North Carolina State University

Raleigh, North Carolina, USA

Manuscript submitted to

Atmospheric Science Letters

Abstract

A high resolution, regional coupled air-sea model is used to investigate the effect of the Gulf Stream (GS) on surface wind convergence during winter extratropical cyclone (ETC) outbreaks in January 2005 off the east coast United States. Validations against marine buoy observed surface wind, sea level pressure (SLP), air temperature, and sea surface temperature (SST) demonstrate decent model skill. Model analyses indicate that the surface wind convergence and the Laplacian of SLP and SST are proportionate on the synoptic time scale. Strong upward vertical motions and ocean heat loss over the GS support rapid ETC intensification.

1. Introduction

The Gulf Stream (GS) is a warm (>24 °C in winter) western boundary current that flows northeastward along the eastern North America continental margin. In winter strong heat flux and surface winds associated with the sharp GS horizontal ocean temperature gradients cause energetic air-sea interactions, rapidly influencing the marine atmospheric boundary layer (MABL) and development of synoptic storms [*Song et al.*, 2006; *Small et al.*, 2008]. During January in particular, frequent (2-4 per month) and intense (average maximum winds of 23 m s^{-1}) winter extratropical cyclones (ETC) form within or just north of the Gulf Stream near Cape Hatteras and track along the northeast coast of the United States [*Colucci*, 1976; *Zishka and Smith*, 1980; *Hirsch et al.*, 2001]. While it is known that such rapidly intensifying east coast ETCs develop offshore along the leading edge of a cold, dry air mass, near the strongest sea surface temperature (SST) gradients, and in regions of surface convergence and upper level divergence [*Sanders and Gyakum*, 1980], quantitative understanding of air-sea interactions during intense winter ETCs has been hindered due to the lack of high-resolution observations that can resolve both temporal and spatial variability of ETCs. In this regard, the Genesis of Atlantic Lows Experiment (GALE) of winter 1986 was the largest field program ever conducted [*Dirks et al.*, 1988]. Concurrent atmospheric and oceanic datasets collected during GALE were used in several observational [*Bane and Osgood*, 1989; *Doyle and Warner*, 1990; *Holt and Raman*, 1990] and modeling [*Huang and Raman*, 1988; *Raman and Reddy*, 1996; *Xue et al.*, 2000] studies to understand air-sea interaction processes important for rapid winter cyclone development.

Coupled air-sea modeling has been long recognized as an important and effective means for studying the mechanisms controlling rapid ETC intensification in data sparse regions. *Xue et al.* [2000] coupled a two-dimensional atmospheric model with a two-dimensional ocean model and found large surface heat fluxes and locally enhanced winds off the southeastern U.S. in a cold air outbreak observed during GALE. That work shows surface winds increase by as much as 75% over the Gulf Stream which has a significant impact on the upper ocean temperature and velocity fields. *Li et al.* (2002) used a three-dimensional coupled model to investigate spatial heat flux patterns during the passage of a winter storm and found that the central pressure dropped sharply as the cyclone encountered the large heat flux gradients at the shoreward side of the Gulf Stream. Recent studies by *Minobe et al.* [2008, 2010] aimed to elucidate the Gulf Stream's influence on the surface wind field. Utilizing QuikSCAT satellite wind data and ECMWF model output, these studies show the mean surface wind convergence on both seasonal and annual time scales exhibits coherent structures along the Gulf Stream, a result that is further corroborated by *Joyce et al.* [2009]. The temporal mean of surface wind convergence is stronger in winter than summer. The atmospheric response to GS-induced surface convergence is confined to the MABL in winter but reaches to the tropopause in summer.

To complement these earlier wind convergence analyses on seasonal and annual time scales, we apply here a newly developed high resolution, regional coupled air-sea model to simulate winter ETC outbreaks in January 2005 and assess wind field adjustments over the Gulf Stream on the synoptic time scale. We describe the configuration of the coupled model

and model validations in Section 2. Section 3 presents detailed wind convergence analysis followed by summary and conclusions in Section 4.

2. Model and Data

2.1 Coupled Air-Sea Model

We used the Coupled-Ocean-Atmosphere-Wave-Sediment-Transport (COAWST) model, which is a newly developed system designed for studying physical interaction processes that effect environmental changes in coastal oceans [*Warner et al.*, 2010]. The COAWST configuration is comprised of the Weather Research and Forecasting (WRF) atmospheric model [*Skamarock et al.*, 2008] and the Regional Ocean Modeling System (ROMS) ocean circulation model [*Shchepetkin and McWilliams*, 2005]. Data exchange between concurrent WRF and ROMS simulations is handled by the Model Coupling Toolkit (MCT) [*Larson et al.*, 2005]. Time steps for WRF and ROMS are 60 and 300 seconds, respectively. During the simulation, wind stress and net heat flux generated by WRF and SST by ROMS are exchanged on each coupling time interval, which is 600 seconds.

The coupled simulation runs from 13-31 January 2005, during which time four east coast ETCs and one "bomb" (defined by *Sanders and Gyakum* [1980] as a surface cyclone with a decrease in sea level pressure of at least 1 mb hr^{-1} for 24 hours) ETC occurred. The model domain encompasses central and eastern North America, the Gulf of Mexico, and the northwestern Atlantic Ocean (**Figure 1**). Given that the strongest ETCs formed just offshore of the east coast of the United States, the model analysis is focused over the western Atlantic Ocean centered at Cape Hatteras, NC. The WRF grid has 15-km horizontal resolution and 48

vertical terrain-following levels from sea level to 100 mb. The ROMS grid is configured with 5-km horizontal resolution and 18 vertical terrain-following levels. The Spherical Coordinate Remapping and Interpolation Package [SCRIP; *Jones*, 1998] program included in COAWST is used to create interpolation weights between the different model grids. Once the weights are computed, wind stress and net heat flux from WRF are interpolated to the ROMS grid and SST from ROMS is interpolated to the WRF model grid. Initial conditions and boundary information for WRF are provided by the 32-km, 3-hour NCEP North American Regional Reanalysis (http://www.esrl.noaa.gov/psd/data/gridded/data.narr.html) data, whereas initial and boundary conditions for ROMS are obtained from the 10-km, daily HYCOM/NCODA global ocean model simulation (http://www.hycom.org/dataserver).

Examinations of marine meteorological buoy time series (*Nelson and He*, submitted) indicate during the first half of January 2005 (1-12 January), calm southerly winds prevailed with mild air temperatures that were about the same as the ocean temperature. In contrast, the second half of month (13-31 January) was characterized by strong ETCs, cold air outbreaks with sharp drops (up to 20 ^{o}C) in surface air temperature, a steady decrease in sea surface temperature up to 5 °C, and large sensible and latent heat fluxes out of the ocean (in excess of 600 W m^{-2} total flux in the storm track). Our study is intended to highlight the stormy second half of the month in order to understand the dynamics involved in the strong air-sea interactions in the study area.

2.2 Model Validation

In-situ observations of near-surface winds, sea level pressure (SLP), air temperature, and sea surface temperature (SST) measured by the National Data Buoy Center (NDBC) buoys 44009, 41001, and 41004 were utilized to validate the coupled model simulation. These in-situ data were sub-sampled every three hours to be concurrent with the coupled model output over the time period 13-31 January 2005. These buoys measure three distinct ocean regions (**Figure 1**): the cold mid-shelf waters north of Cape Hatteras (buoy 44009), the seaward side of the Gulf Stream offshore of Cape Hatteras (buoy 41001), and the warm mid-shelf waters south of Cape Hatteras (buoy 41004). Each model-data wind time series comparison is quantified by a vector correlation coefficient (r), the vector orientation difference (Θ) between observed and model-simulated winds (measured in degrees counterclockwise from true north), and a vector regression coefficient. The remaining comparisons are quantified by their correlation coefficient (r) and root mean square error (RMS error).

The coupled model simulation reproduces observations well. The correlation coefficients (**Table 1**) between observed and modeled winds range from 0.84-0.93. Modeled wind orientations agree to between -2.5° and -9.0° with near-perfect amplitudes (regression coefficients being 0.91-1.06). The correlations for SLP are 0.98 or higher with mean offsets of less than 1.70 hPa. The air temperature comparisons are also good at all stations, with correlations 0.96 or better and mean offsets less than 2.7 °C. We note the buoy air temperature sensors have a cold bias due to ocean surface evaporation resulted from storm-induced wave breaking [*J. Bane*, personal communication], which explains at least in part the

~2.5 °C offset between buoy-observed and model-simulated air temperature. SST comparisons are reasonable as well except at buoy 41004. At that location, small lateral movements of the Gulf Stream are not captured by the 5-km resolution ocean model, resulting in a low correlation at this station. Nevertheless, SST time series are highly correlated (>0.96) with less than 0.6 °C bias at the other two stations (44009 and 41001). Based on these and other (not shown) favorable comparisons, we conclude that our coupled model produced realistic simulations of oceanic and atmospheric conditions during the ETC outbreaks in January 2005, lending confidence that dynamical analysis described below is couched in a realistic air-sea environment.

3. Model Analysis

With temporally and spatially continuous model fields, we begin by analyzing the synoptic mean surface wind convergence during the ETC outbreak from 13-31 January 2005 (**Figure 2a**). Surface wind convergence is calculated as $-(u_x + v_y)$, where u and v are the mean 10-m eastward and northward wind velocity components, respectively. A broad band of convergence is seen off the southeastern U.S. coast aligned with the 19 °C isotherm (e.g. Gulf Stream SST front), comparing nicely to the spatial distributions of the annual and seasonal (December-January-February) mean convergence given by *Minobe et al.* [2008, 2010]. The convergence maxima are an order of magnitude stronger than the seasonal mean convergence observed by *Minobe et al.*, [2010], and located where the strong northerly winds off the continent first encounter the SST front over the warm Gulf Stream waters. We also

note a smaller local convergence zone over the Middle Atlantic Bight (MAB) shelfbreak where a shelfbreak front is known to exist [*Linder and Gawarkiewicz,* 1998].

To understand the mechanism that drives synoptic wind convergence along the Gulf Stream, we examine a simple, linear theoretical model based on geostrophic and Ekman dynamics proposed by *Minobe et al.* [2008]:

$$\varepsilon u - fv = -P_x/\rho_0 \qquad (1)$$

$$\varepsilon v + fu = -P_y/\rho_0 \qquad (2)$$

where u and v are the 10-m across-shelf and along-shelf velocity components, P is sea level pressure, ε is a constant frictional damping coefficient, f is the Coriolis parameter, and ρ_0 is the air density. Using the mathematical convention where a single subscript indicates a partial derivative and a double subscript is the second derivative, we can obtain the following by taking the derivative with respect to x and y of equation 1 to obtain:

$$\varepsilon u_x - fv_x = -P_{xx}/\rho_0 \qquad (3)$$

$$\varepsilon u_y - fv_y = -P_{xy}/\rho_0 \qquad (4)$$

and of equation 2 to obtain:

$$\varepsilon v_x + fu_x = -P_{xy}/\rho_0 \qquad (5)$$

$$\varepsilon v_y + fu_y = -P_{yy}/\rho_0 \qquad (6)$$

Addition of equations 3 and 6 results in:

$$\varepsilon(u_x + v_y) + f(u_y - v_x) = -(P_{xx} + P_{yy})/\rho_0 \qquad (7)$$

By subtracting equation 5 from equation 4, we can eliminate the $-P_{xy}$ terms and are left with:

$$\varepsilon(u_y - v_x) - f(v_y + u_x) = 0 \qquad (8)$$

Equation 8 can be rearranged to solve for $(u_y - v_x)$ so that $(u_y - v_x) = f/\varepsilon(u_x + v_y)$. A simple substitution of $(u_y - v_x)$ into equation 7 gives:

$$\varepsilon(u_x + v_y) + f^2/\varepsilon(u_x + v_y) = -(P_{xx} + P_{yy})/\rho_0 \qquad (9)$$

Finally, by combining the convergence terms in equation 9 and reorganizing the remaining terms we come up with:

$$-(u_x + v_y)\,\rho_0 = (P_{xx} + P_{yy})\,\varepsilon/(\varepsilon^2 + f^2) \qquad (10)$$

which as *Minobe et al*. [2008] indicates, shows that surface wind convergence is proportional to the Laplacian of SLP.

Lindzen and Nigam [1987] shows that the relationship between SST and SLP can be approximated by: $P = g\rho_0 n H_0(\gamma/2 - 1)T$, where T is the SST, P is the SLP, γ is a constant, g is gravitational acceleration, H_0 is the equivalent depth of the atmosphere, and n is the local derivative of air density over temperature $-(\frac{1}{\rho}\frac{\partial\rho}{\partial T})$. Since this equation indicates that SLP is linearly forced by SST, it can be further deduced that surface wind convergence is also proportional to the Laplacian of SST, that is: $-(u_x + v_y)\rho_0 \sim -(T_{xx} + T_{yy})$.

Indeed the spatial patterns of the synoptic mean SLP Laplacian (**Figure 2b**) are strikingly similar to the mean surface wind convergence (**Figure 2a**), particularly in the breadth of the convergence zone and the meandering along the 19 °C isotherm associated with the mean position of the Gulf Stream SST front. Positive SLP Laplacian, indicating pressures that are lower than the surrounding mean pressure, shows excellent correspondence to the surface wind convergence zone. Point-by-point comparisons indicate the mean wind convergence is linearly related to SLP Laplacian with a correlation of 0.82 (**Figure 2d**).

Likewise, the relationship between the mean surface wind convergence and mean sign-reversed SST Laplacian (representing where SST has dropped more than the adjacent mean ocean temperature) is pronounced over the coastal areas and along the length of the GS front. Although this correspondence begins to break down further offshore, the linear relationship is still maintained with a positive correlation of 0.52 over the entire study domain (**Figure 2e**).

This analysis suggests that the air-sea interactions over the Gulf Stream during a winter storm outbreak quickly modify the overlying atmospheric temperature, pressure, and wind fields. Initially, the ocean loses heat to the atmosphere primarily along the length of the Gulf Stream front due to persistent cooling associated with the passage of ETCs. Heat fluxes warm the MABL and generate an area of relatively low pressure offshore. Low SLP anomalies cause surface winds to accelerate offshore and converge over the Gulf Stream.

To further illustrate the dynamic coupling between the ocean and atmosphere during east coast ETC outbreaks, we examine vertical profiles of synoptic mean vertical wind velocities from sea level to 800 mb in relation to –SST Laplacian and SLP Laplacian along three cross-shelf transects (**Figure 3**). Transects T1-3 span the cool waters of the northern MAB shelf, the Gulf Stream near Cape Hatteras, and the Gulf Stream in the South Atlantic Bight (SAB), respectively (see their locations in the inset panel of Figure 1). Lateral distributions of vertical motions in the MABL correspond well with the along-transect Laplacian of SLP and –SST. The stronger, more-defined upward motions, indicated by positive vertical velocity, are aligned with maximum SLP Laplacian, while weaker vertical velocities are co-located with peaks in –SST Laplacian, particularly over the Gulf Stream

SST front about 50-100 km from the shoreward end of transects T2 and T3. Based on the relationship between surface wind convergence and SLP Laplacian, our analysis suggests that the upward vertical motions anchored over the Gulf Stream (T2 and T3) are triggered by strong surface convergence.

4. Summary and Conclusion

We utilize a high resolution, regional scale air-sea coupled model (WRF/ROMS configuration of the COAWST modeling system) to simulate five east coast ETCs from 13 to 31 January 2005. Very good agreements are found between buoy-observed and model-simulated surface winds, SLP, air temperature, and SST. Coupled model diagnostics reveal a clearly defined band of maximum surface wind convergence co-located with the warm Gulf Stream waters. Complementary to *Minobe et al.* [2008, 2010] studies on the Gulf Stream effect on seasonal and annual mean wind convergence, our study shows that surface wind convergence and the Laplacian of SLP and Laplacian of –SST are proportionate even on the synoptic time scale. Strong air-sea interactions during winter ETC outbreaks, particularly the low SLP anomalies offshore and enhanced ocean heat loss, generate the Gulf Stream surface wind convergence zone and the subsequent upward motions throughout the MABL, supporting rapid ETC intensification off the eastern U.S. seaboard.

It can be concluded that in order to improve ETC predictions and regional coastal wind and wind energy potential assessment in general, such strong air-sea interactions affecting momentum and buoyancy flux exchanges have to be accurately accounted for in an atmosphere-ocean coupled modeling framework.

Acknowledgements

We are grateful to research funding support provided by NSF and ONR through grants OCE-0927470 and N00014-06-1-0739, respectively. We thank Dr. J. Warner of USGS for productive collaboration and leading the effort in developing and testing the COAWST modeling system, and Dr. J. Bane of UNC for scientific guidance and many enlightening discussions. Z. Yao's assistance in setting up the ocean model is appreciated. Results analyses presented here are part of J. Nelson master's thesis research at North Carolina State University.

REFERENCES

Bane, J. M., and K. E. Osgood (1989), Wintertime air-sea interaction processes across the Gulf Stream, *J. Geophys. Res.*, *94*, 10755-10772.

Colucci, S. J. (1976), Winter cyclone frequencies over the eastern United States and adjacent western Atlantic, 1964-1973, *Bull. Am. Meteor. Soc.*, *57*(5), 548-553.

Dirks, R. A., J. P. Kuettner, and J. A. Moore (1988), Genesis of Atlantic Lows Experiment (GALE): An overview, *Bull. Am. Meteor. Soc.*, *69*(2), 148-160.

Doyle, J. D., and T. T. Warner (1990), Mesoscale coastal processes during GALE IOP 2, *Mon. Weather Rev.*, *118*, 283-308.

Hirsch, M. E., A. T. DeGaetano, and S. J. Colucci (2001), An east coast winter storm climatology, *J. Climate*, *14*, 882-899.

Holt, T. R., and S. Raman (1990), Marine boundary-layer structure and circulation in the region of offshore redevelopment of a cyclone during GALE, *Mon. Weather Rev.*, 120, 17-39.

Huang, C.-Y., and S. Raman (1988), A numerical modeling study of the marine boundary layer over the Gulf Stream during cold air advection, *Bound.-Layer Meteor.*, *45*, 251-290.

Jones, P. W. (1998), A user's guide for SCRIP: A Spherical Coordinate Remapping and Interpolation Package. Los Alamos National Laboratory. WWW page: http://climate.lanl.gov/Software/SCRIP/.

Joyce, T. M., Y.-O. Kwon, and L. Yu (2009), On the relationship between synoptic wintertime variability and path shifts in the Gulf Stream and the Kuroshio Extension, *J. Climate*, *22*, 3177-3192.

Larson J., R. Jacob, and E. Ong (2005), The Model Coupling Toolkit: A new FORTRAN90 toolkit for building multiphysics parallel coupled models. *Int. J. High Perform. C.*, *19*, 277-292.

Linder, C. A., and G. Gawarkiewicz (1998), A climatology of the shelfbreak front in the Middle Atlantic Bight, *J. Geophys. Res.*, *103*, 18405-18423.

Lindzen R. S., and S. Nigam (1987), On the role of sea surface temperature gradients in forcing low-level winds and convergence in the tropics, *J. Atmos. Sci.*, *44*(7), 2418-2436.

Li, Y., H. Xue, and J. M. Bane (2002), Air-sea interactions during the passage of a winter storm over the Gulf Stream: A three-dimensional coupled atmosphere-ocean model study, *J. Geophys. Res.*, *107*, 1-13.

Minobe, S., A. Kuwano-Yoshida, N. Komori, S.-P. Xie, and R. J. Small (2008), Influence of the Gulf Stream on the troposphere, *Nature*, *452*, 206-210, doi:10.1038/nature06690.

Minobe, S., M. Miyashita, A. Kuwano-Yoshida, H. Tokinaga, and S.-P. Xie (2010), Atmospheric response to the Gulf Stream: Seasonal variations, *J. Climate*, *23*, 3699-3719, doi:10.1175/2010JCLI3359.1.

Nelson, J. S. and R. He, submitted, Air-sea interactions during strong winter extratropical storms, *Dyn. Atmos. Oceans*

Raman, S., and N. C. Reddy (1996), Numerical simulation of a mesolow over a Gulf Stream Filament, *Pure Appl. Geophys.*, *147*, 789-819.

Sanders, F., and J. R. Gyakum (1980), Synoptic-dynamic climatology of the "bomb", *Mon. Weather Rev.*, *108*, 1589-1606.

Shchepetkin, A. F., and J. C. McWilliams (2005), The Regional Ocean Modeling System: A split-explicit, free-surface, topography-following coordinates ocean model, *Ocean Modell.*, *9*, 347–404.

Skamarock, W. C., J. B. Klemp, J. Dudhia, D. O. Gill, D. M. Barker, M. G. Duda, X.-Y. Huang, W. Wang, and J. G. Powers (2008), A description of the Advanced Research WRF Version 3, Technical note, National Center for Atmospheric Research, TN-475+STR, WWW page: http://www.mmm.ucar.edu/wrf/users/docs/arw_v3.pdf.

Small, R. J., S. P. deSzoeke, S. P. Xie, L. O'Neill, H. Seo, Q. Song, P. Cornillon, M. Spall, and S. Minobe (2008), Air-sea interactions over ocean fronts and eddies, *Dyn. Atmos. Oceans*, *45*, 274-319.

Song, Q., P. Cornillon, and T. Hara (2006), Surface wind response to oceanic fronts, *J. Geophy. Res.*, 111, C12006.

Warner, J. C., B. Armstrong, R. He, and J. B. Zambon (2010), Development of a Coupled-Ocean-Atmosphere-Wave-Sediment-Transport (COAWST) modeling system, *Ocean Modell.*, *35*, 230-244, doi:10.1016/j.ocemod.2010.07.010.

Xue, H., Z. Pan, and J. M. Bane (2000), A 2D coupled atmosphere-ocean model study of air-sea interactions during a cold air outbreak over the Gulf Stream, *Mon. Weather Rev.*, *128*, 973-996.

Zishka, K. M., and P. J. Smith (1980), The climatology of cyclones and anticyclones over North America and surrounding ocean environs for January and July, 1950-77, *Mon. Weather Rev.*, *108*(4), 387-401.

TABLES

Table 1. Statistic measures of time series comparisons between observed and simulated wind vectors, sea level pressure (SLP), air temperature (T), and sea surface temperature (SST) at marine buoys 44009, 41001, and 41004

Buoy	Wind Comparisons	SLP Comparisons	T Comparisons	SST Comparisons
	r / Θ / regression	r / RMS Error		
44009	0.92 / -2.5 / 1.06	0.99 / 1.45	0.96 / 1.96	0.97 / 0.59
41001	0.84 / -3.9 / 0.91	0.98 / 1.70	0.97 / 2.69	0.96 / 0.47
41004	0.93 / -9.0 / 0.99	0.98 / 1.62	0.96 / 2.65	0.02 / 1.75

FIGURES

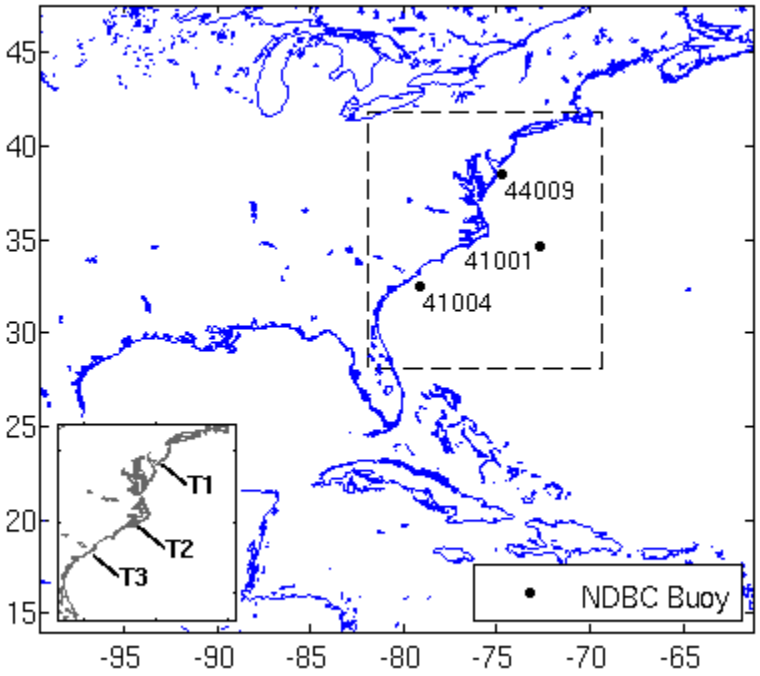

Figure 1. The model domain for the coupled WRF and ROMS simulation (outermost box). The dashed box highlights our east coast study region. Also shown are locations of three NDBC marine buoys and three cross-shelf transects (bottom left inset panel) along which vertical profiles of MABL wind fields are diagnosed.

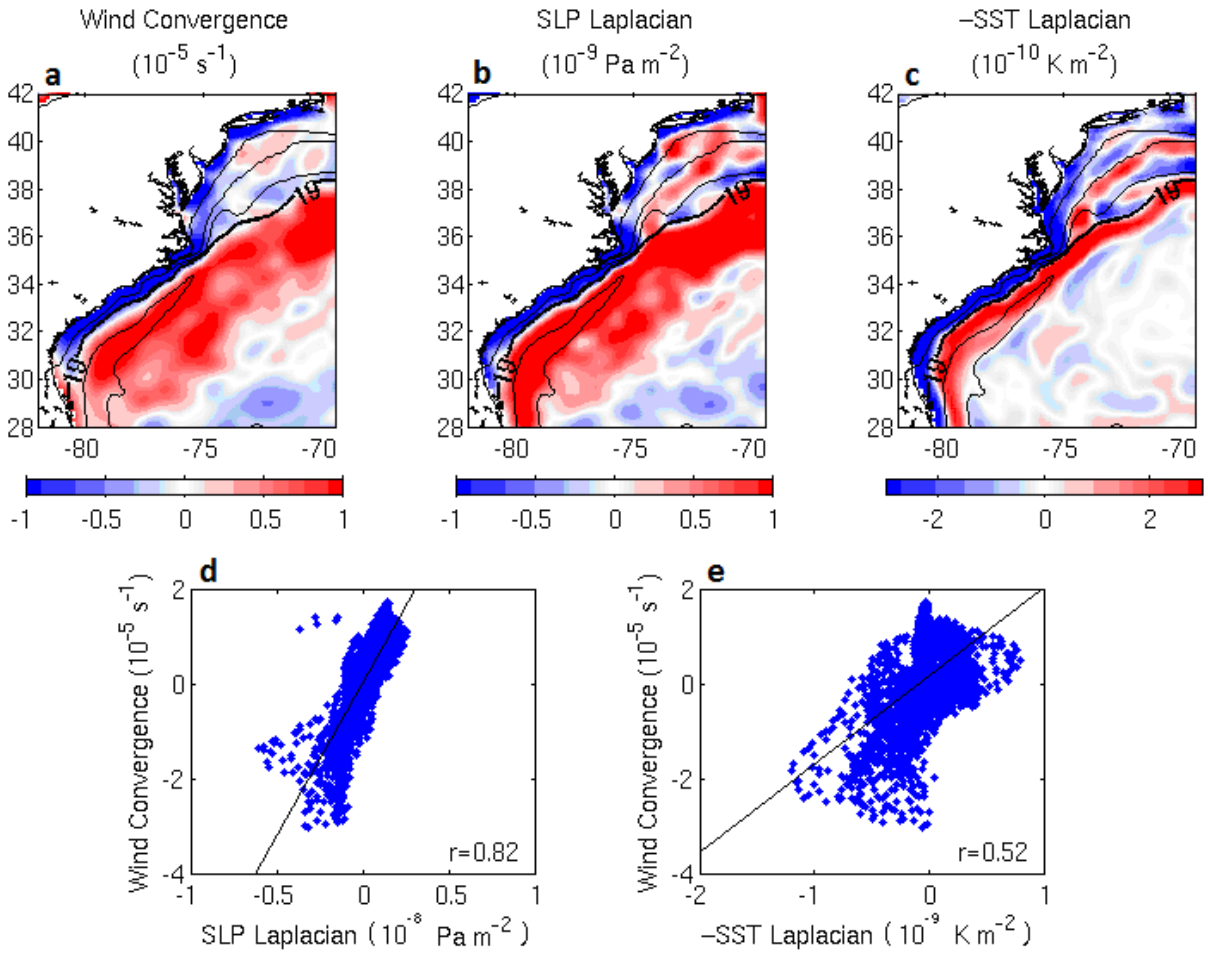

Figure 2. Simulated synoptic mean (averaged over 13-31 January 2005) 10-m wind convergence (a), mean SLP Laplacian (b), and mean SST Laplacian with the sign reversed (c). Contours on (a)—(c) are for mean SST (4 °C interval). Also presented are the point-to-point comparisons between mean wind convergence and mean SLP Laplacian (d), and between mean wind convergence and –SST Laplacian (d). In both (d) and (e), the linear regression line and its corresponding correlation coefficient are given.

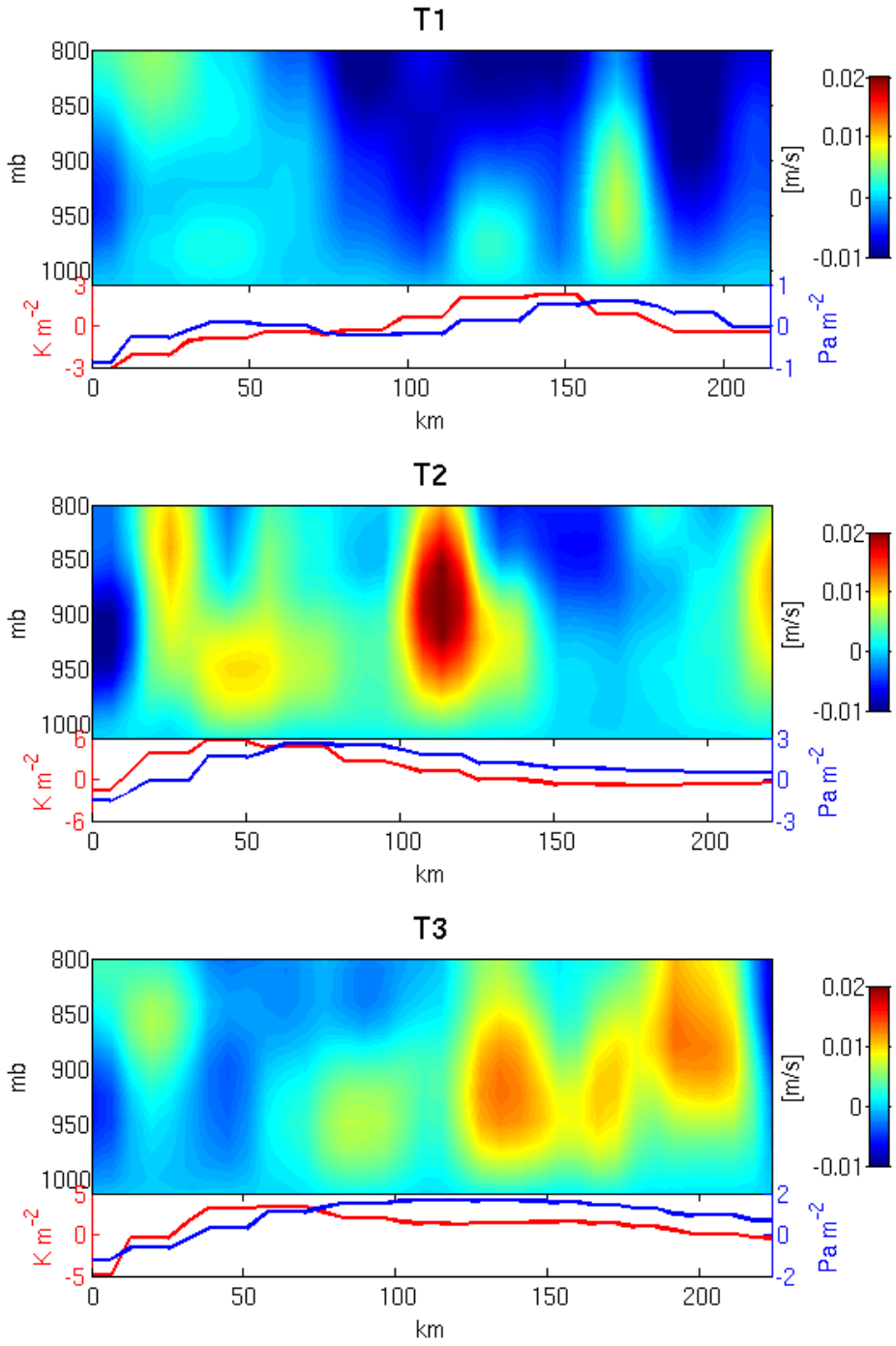

Figure 3. Vertical profiles of simulated synoptic mean wind vertical velocity (shaded; upward positive, m s^{-1}) along three cross-shelf transects (locations of T1, T2, and T3 shown in Figure 1). Also shown at the bottom of each panel are along-transect –SST Laplacian (red; 10^{-10} K m^{-2}) and SLP laplacian (blue; 10^{-9} Pa m^{-2}).

CHAPTER 4

Summary and Conclusions

Regional coupled atmosphere-ocean models have been shown to be quite effective for studying energetic air-sea interactions during rapidly developing marine extratropical cyclones (ETCs) [e.g. *Li et al.*, 2002; *Xue et al.*, 1995, 2000]. Complex feedbacks between the marine atmospheric boundary layer (MABL) and the upper ocean within winter ETCs are resolved by time and space continuous model fields. To this end, the Coupled-Ocean-Atmosphere-Wave-Sediment-Transport (COAWST) modeling system was utilized for simulating the January 2005 ETC outbreak off the east coast of the United States. In the COAWST configuration for this thesis research, the Weather Research and Forecasting (WRF) atmosphere model was coupled with the Regional Ocean Modeling System (ROMS), whereby wind stress and net heat flux generated by WRF every minute and sea surface temperature (SST) generated by ROMS every five minutes were exchanged simultaneously every ten minutes during the hindcast simulation.

Model simulations were run from 13-31 January 2005, encompassing an outbreak of five strong extratropical cyclones off the U.S. east coast including one particularly intense "bomb" ETC on 22-23 January (defined by *Sanders and Gyakum* [1980] as a cyclone with surface central pressure decreases of at least 1 mb an hour for 24 hours). Hourly measurements made off the Delaware coast by National Data Buoy Center (NDBC) buoy 44009 during the outbreak indicated large drops in air and ocean temperatures (20 °C and 5 °C, respectively) and excessive sensible and latent heat fluxes (up to 600 W m^{-2}) out of the

ocean with each system. The coupled model performed well compared to the hourly time series of surface winds, sea level pressure, air temperature, and SST measured by three NDBC buoys from 13-31 January 2005. The modeled subsurface temperature structures also compared favorably to the Rutgers University glider survey of the northern Middle Atlantic Bight (MAB) shelf on 14 January 2005. These agreeable coupled model validations permitted confidence in the analyses presented in Chapters 2 and 3 of this thesis.

Detailed analyses of the air-sea interactions and oceanic heat budget for the 22-23 January 2005 "bomb" ETC were discussed in Chapter 2 of this thesis. An area of low pressure seen off Cape Hatteras, NC, on 22 January intensified into a mature cyclone (deepening 24 mb in 24 hours) as it tracked northeastward across the Atlantic Ocean. Extreme cold and high wind conditions persisted over the ocean for several days following the cold front. Vertical profiles of the MABL up to 800 mb and the ocean down to 100 m along three cross-shelf transects illustrated the air mass modification during the storm's passage as well as the upper ocean response during the cold air outbreak. During the pre-storm phase and the cold front passage, the convergence of warm air at the surface induced upward winds and rapid MABL heating of 10-15 °C. Behind the cold front, strong storm winds and large air-sea temperature and humidity differences generated up to 1000 W m^{-2} total ocean-to-atmosphere heat flux over the Gulf Stream which cooled the upper ocean by 2 °C. The ocean response was consistent with that observed by *Bane and Osgood* [1989] and *Xue et al.* [1995] over the Gulf Stream during the Genesis of Atlantic Lows Experiment in winter 1986. The ocean heat budget was quantified along the same three cross-shelf transects to diagnose the processes which resulted in a ~2 °C temperature loss in the upper

(0-100 m) ocean. On the shallow MAB shelf, surface heat flux out of the ocean and ocean advection controlled the upper ocean temperature variations during the storm period. Near the Gulf Stream, the cooling due to excessive ocean-to-atmosphere surface heat fluxes during the cold air outbreak was partially counteracted by the warming effect of ocean heat advection.

Chapter 3 of this thesis addressed the Gulf Stream's impact on synoptic mean surface wind convergence over the entire 13-31 January 2005 ETC outbreak. Recent studies by *Minobe et al*. [2008, 2010] show the mean surface wind convergence on seasonal and annual time scales exhibits coherent structures along the Gulf Stream. In this thesis, surface wind convergence was calculated as $-(u_x + v_y)$, with u and v being the mean 10-m eastward and northward wind velocity components obtained from the two-way coupled model run. Model diagnostics showed a broad band of convergence off the southeastern U.S. coast aligned with the Gulf Stream SST front, complementing the spatial distributions of the annual and wintertime (December-January-February) mean convergence given by *Minobe et al.* [2008, 2010]. Surface wind convergence was shown to be proportional to the Laplacian of sea level pressure (SLP) and the inverse Laplacian of sea surface temperature based on *Lindzen and Nigam's* [1987] theoretical MABL model. These results indicated a systematic process by which the Gulf Stream induces convergence. The passage of strong cold fronts causes a steady SST decrease, particularly across the Gulf Stream, where air pressures fall rapidly with the addition of heat and moisture to the MABL. Locally enhanced surface winds associated with the low pressure anomaly generate the surface wind convergence zone over

the Gulf Stream. Strong upward vertical motions throughout the MABL (up to 800 mb) were triggered by the surface wind convergence during the ETC outbreak.

Two model sensitivity simulations were performed in addition to the *two-way coupled run* (WRF/ROMS configuration described above) to demonstrate the importance of air-sea coupling during winter extratropical cyclones, including the *one-way coupled run* (WRF-only simulation with a low-resolution SST linearly interpolated every three hours) and the *uncoupled run* (WRF-only simulation with a time-invariant SST from 13 January 2005). The two-way coupled simulation had a strong correlation between surface wind convergence and the Laplacian of SLP and the inverse Laplacian of SST (0.82 and 0.52, respectively), whereas the one-way coupled and uncoupled runs had much weaker correlations to the Laplacian of SLP and SST. This result provides clear evidence that the feedbacks between the MABL and the upper ocean during winter storms are best represented by the two-way coupled model where the ocean can respond to atmospheric changes it induced and vice versa. It can be concluded that in order to improve winter ETC and regional coastal wind predictions, dynamic air-sea interactions affecting momentum and buoyancy flux exchanges have to be accurately accounted for in a coupled atmosphere-ocean modeling framework.

REFERENCES

Bane, J. M., and K. E. Osgood (1989), Wintertime air-sea interaction processes across the Gulf Stream, *J. Geophys. Res.*, *94*, 10755-10772.

Lindzen R. S., and S. Nigam (1987), On the role of sea surface temperature gradients in forcing low-level winds and convergence in the tropics, *J. Atmos. Sci.*, *44*(7), 2418-2436.

Li, Y., H. Xue, and J. M. Bane (2002), Air-sea interactions during the passage of a winter storm over the Gulf Stream: A three-dimensional coupled atmosphere-ocean model study, *J. Geophys. Res.*, *107*, 1-13.

Minobe, S., A. Kuwano-Yoshida, N. Komori, S.-P. Xie, and R. J. Small (2008), Influence of the Gulf Stream on the troposphere, *Nature*, *452*, 206-210, doi:10.1038/nature06690.

Minobe, S., M. Miyashita, A. Kuwano-Yoshida, H. Tokinaga, and S.-P. Xie (2010), Atmospheric response to the Gulf Stream: Seasonal variations, *J. Climate*, *23*, 3699-3719, doi:10.1175/2010JCLI3359.1.

Sanders, F., and J. R. Gyakum (1980), Synoptic-dynamic climatology of the "bomb", *Mon. Weather Rev.*, *108*, 1589-1606.

Xue, H., J. M. Bane, and L. M. Goodman (1995), Modification of the Gulf Stream through strong air-sea interactions in winter: Observations and numerical simulations, *J. Phys. Oceanogr.*, *25*, 533-557.

Xue, H., Z. Pan, and J. M. Bane (2000), A 2D coupled atmosphere-ocean model study of air-sea interactions during a cold air outbreak over the Gulf Stream, *Mon. Weather Rev.*, *128*, 973-996.